الجمهورية الجزائرية الديمقراطية الشعبية
Democratic and Popular Republic of Algeria
وزارة التعليم العالي والبحث العلمي
Ministry of Higher Education and Scientific Research
جامعة غرداية
University of Ghardaïa

N° registration
/…../…../…../…../…..

كلية العلوم والتكنولوجيا
Faculty of Science and Technology
قسم الآلية والكهروميكانيك
Department of Mechanics and Electro mechanics

Final year dissertation, with a view to obtaining the diploma

Master

Domain : Science and Technology
Sector : Mechanical Engineering
Specialty : Renewable energies in mechanics

Theme

Comparative analysis of three solar dryer configurations based on temperature distribution in the drying chamber

Presented by: DERBALI Yahia & LAOUAR Tamer

Publicly supported the: 12/06/2025

Before the jury composed of:

BAHRI Ahmed		**Univ. Ghardaïa**	**President**
Dr. HAKIM MERARDA	**Research Master B**	**URAER-CDER**	**Supervisor**
BENSEDDIK Abdelouahab	**Research Master A**	**Univ. Ghardaïa**	**Examiner**
KHLIFI Rezki			**Examiner**

Academic year 2024/2025

ملخص

كجزء من دراستنا، تمت محاكاة ثلاثة تصاميم مختلفة لمجففات الطاقة الشمسية غير المباشرة باستخدام أدوات محاكاة التدفق في SolidWorksلتقييم أدائها الحراري في ظل ظروف مناخية مختلفة. تم تقييم الأنظمة، المكونة من مجمع واحد ومجمعين وثلاثة مجمعات، باستخدام برنامج Mathlab في ثلاثة تواريخ شمسية رئيسية: 21 مارس و21 يونيو و21 ديسمبر. قمنا بحساب زوايا ارتفاع الشمس وسمتها عند نقطتين زمنيتين حرجتين - 10:00 صباحًا وظهرًا - لاستخدامها في عمليات المحاكاة. كشفت عمليات المحاكاة أن زيادة عدد المجمعات يعزز بشكل كبير الكفاءة الحرارية للنظام، وخاصة خلال فترة الظهيرة عندما يكون الإشعاع الشمسي في ذروته. على الرغم من اختلاف درجات الحرارة المحيطة عبر التواريخ المدروسة، إلا أن الإشعاع العمودي المباشر (DNI)كان له التأثير الأكبر على أداء النظام. والجدير بالذكر أن تصميم المجمعات الثلاثة تفوق باستمرار على التكوينات الأخرى، محققًا أعلى كفاءة نسبية في 21 جوان عند الظهر بسبب موقع الشمس و درجة الحرارة الهواء المحيطة. تُظهر هذه النتائج أن تصميمات المجمعات المتعددة توفر كفاءة تجفيف فائقة، وتؤكد على أهمية تحسين مساحة المجمع بناءً على الظروف الشمسية المحلية والاحتياجات التشغيلية.

الكلمات المفتاحية: مجفف شمسي غير مباشر: الإشعاع الطبيعي المباشر (DNI) : محاكاة تدفق سوليدووركس.

Résumé

Dans le cadre de notre étude, trois conceptions différentes de séchoirs solaires indirects ont été simulées à l'aide des outils de simulation d'écoulement SolidWorks afin d'évaluer leurs performances thermiques dans diverses conditions climatiques. Les systèmes, composés d'un, deux et trois capteurs, ont été évalués à l'aide du logiciel Mathlab à trois dates solaires clés : les 21 mars, 21 juin et 21 décembre. Nous avons calculé les angles d'élévation et d'azimut du soleil à deux moments critiques, 10 am et midi, pour les simulations. Ces dernières ont révélé qu'une augmentation du nombre de capteurs améliore significativement l'efficacité thermique du système, en particulier en milieu de journée, lorsque le rayonnement solaire est à son maximum. Bien que les températures ambiantes aient varié selon les dates étudiées, l'irradiance normale directe (DNI) a eu l'impact le plus important sur les performances du système. Il est à noter que la conception à trois collecteurs a systématiquement surpassé les autres configurations, atteignant l'efficacité relative la plus élevée le 21 juin à midi en raison de la position du soleil et de la température de l'air ambiant. Ces résultats démontrent que les conceptions à plusieurs collecteurs offrent une efficacité de séchage supérieure et soulignent l'importance d'optimiser l'espace des collecteurs en fonction des conditions solaires locales et des besoins opérationnels.

Mots-clés : séchoir solaire indirect : irradiance normale directe (DNI) : simulation d'écoulement SolidWorks

Abstract

As part of our study, three different indirect solar dryer designs were simulated using SolidWorks flow simulation tools to evaluate their thermal performance under various climatic conditions. The systems, consisting of one, two, and three collectors, were evaluated using the Mathlab software on three key solar dates: March 21st , June 21st , and December 21st . We calculated the sun's elevation and azimuth angles at two critical time points—10:00 a.m. and noon to be used in the simulations. The simulations revealed that increasing the number of collectors significantly enhances the system's thermal efficiency, particularly during the midday period when solar radiation is at its peak. Although ambient temperatures varied across the studied dates, direct normal irradiance (DNI) had the greatest impact on system performance. Notably, the three-collector design consistently outperformed the other configurations, achieving the highest relative efficiency on June 21 at noon due to the position of the sun and the ambient air temperature .These results demonstrate that multi-collector designs provide superior drying efficiency and emphasize the importance of optimizing collector space based on local solar conditions and operational needs.

Keywords:indireect solar dryer: direct normal irradiance (DNI):solidworks flow simullation

THANKS

First of all, I thank Allah for granting me the health and ability to complete my research and project from start to finish.

Secondly, I extend my deepest gratitude to my supervisor, ***researcher and Dr.Hakim Merarda****, for the valuable academic support and guidance he provided throughout the preparation of this dissertation. His expertise, diligence, and generosity greatly influenced my guidance and helped me overcome the challenges and complete this academic project.*

I also extend my sincere thanks and appreciation to the esteemed members of the examination committee for devoting their valuable time to review this work and offering their constructive comments.

I would also like to thank all my esteemed professors during my master's degree and everyone who contributed to my academic and cognitive development throughout my years of study.

I also express my sincere gratitude to my dear family, who have been my support and encouragement throughout this journey, and to all my friends and colleagues who have supported me with their words and encouragement.

My sincere thanks and appreciation to everyone.

DERBALI YAHIA

THANKS

Praise be to God, by whose grace good deeds are accomplished, and by whose grace goals are achieved.

I am pleased to extend my deepest gratitude and appreciation to everyone who supported me and stood by me throughout the completion of this dissertation.

I extend my sincere gratitude and appreciation to Researcher and ***Dr.Hakim Merarda*** *for the valuable guidance, constructive comments, and continuous support he provided throughout the research process. Without his guidance, I would not have reached this conclusion.*

I also cannot fail to extend my deep thanks to all the professors in the Department of Mechanism and electromechanics for their tireless efforts in teaching and academically developing me throughout my studies.

I especially thank my esteemed family, my lifelong supporter, for their moral and material support and constant encouragement. They have my love and gratitude.

I must also not forget to thank my friends and colleagues, who have been my best companions throughout my Master's journey and shared this experience with me, with all its challenges and achievements.

To all of you, much appreciation and thanks

LAOUAR TAMER

List of tables

List of figures

Table of contents

Chapter II:DETERMINATION OF SOLAR POSITION

Chapter III: introduction to Solidworks and fluid flow simulation

General introduction

General introduction

Solar energy represents one of the most promising forms of renewable energy, and its adoption is growing globally. By harnessing the sun's rays—both in the form of light and heat—it offers a clean and sustainable alternative to conventional energy sources. Its flexibility and widespread availability make it a key pillar in the global transition to greener energy systems. A wide range of technologies have emerged to harness solar energy, including photovoltaic panels for electricity generation, solar water heaters, thermal cookers, and solar drying systems. These innovations not only contribute to reducing dependence on fossil fuels and lowering greenhouse gas emissions, but also support broader sustainable development goals. Among these technologies, solar dryers are particularly important. These systems use solar thermal energy to remove moisture from agricultural products such as fruits, vegetables, and grains. Drying has long been used as a preservation method to improve food shelf life, maintain nutritional content, and reduce microbial risks. In light of growing concerns about energy sustainability and global food security, the design and optimization of solar dryers has become increasingly important. Its decentralized nature also enables localized treatment solutions, especially in rural or off-grid areas, while minimizing environmental impact.

This study aims to analyze comparative of three different indirect solar dryer designs, using two programs, Matlab and SolidWorks, to simulate the sun's motion and the thermal behavior of the system, respectively. The focus was on studying the effect of the number of solar collectors on drying efficiency. The results aim to identify the optimal design that achieves the highest thermal efficiency.

- The first chapter provides an overview of solar drying, classifying solar dryers, their components, and various drying methods. It also provides a bibliography that presents experimental and numerical work conducted in the field of solar drying.
- The second chapter is devoted to simulating the sun's position over three days at two different times using the Matlab program.
- The third chapter is devoted to designing various models of indirect solar dryers and simulating them using the SolidWorks program to determine which one has the best efficiency.

Finally, there is a general conclusion summarizing the main findings.

CHAPTRE I :

General Concept About Drying

I. Introduction

Solar drying is one of the oldest methods used by humanity to preserve agricultural products. This process consists of partially or completely removing moisture from a material, whether solid or liquid, in order to obtain a solid final product. It is based on two main phenomena: heat transfer, which allows the phase change of water into vapor, and mass transfer, where water evaporates from the product and diffuses into the surrounding air. The purpose of drying is to reduce the water content of the product, in order to lower its water activity to a level that allows its conservation at room temperature for long periods, up to one year.[1]

The causes of dehydration are divided as follows:

- Facilitate the conservation of products (by reducing water activity).
- Reduce the mass and volume of products to reduce their bulk and facilitate their transport.
- To give a particular presentation, structure or functionality to the product (mashed potato flakes, freeze-dried coffee, etc.).

But the disadvantages of drying are:

- Modification of the product in its form, texture, nutritional and organoleptic qualities.[2]

These phenomena depend on the specific properties of the surrounding gas, whether air or superheated steam, and their intrinsic characteristics.

- Its temperature.
- Its relative humidity.
- its speed.
- Its pressure.[3]

In this first chapter, we will explore the key elements of the most efficient solar collectors for drying. We will examine the various techniques and methods of drying using solar energy, while defining the different types of existing dryers and their specific roles.

I.1 The drying principle:

The drying process is based on two essential mechanisms: heat transfer, which provides the energy needed to evaporate the liquid and mass transfer, which ensures the migration of moisture from the core of the material to its surface before it passes into the gas phase. The efficiency and speed of drying depend directly on the interaction between these two phenomena.[3]

I.2Drying processes:

There are many methods and ways that can be used for drying

I.2.1 Convection drying

This drying process is distinguished by the dual role of air, which ensures both the transfer of heat to the surface of the product, in accordance with Newton's law, and the evacuation of the released water vapor. It is important to emphasize that the circulation of the heat transfer fluid can be done either by natural convection or by forced convection, depending on the needs of the process.[2]

$$Q_{conv} = h * S(Ta - Ts) \quad \text{(I.1)}$$

Q_{conv}: the convection heat flux in $Watt$

h: convection exchange coefficient

$T_{a,}$ and$T_{s,}$: ambient air and product surface temperatures respectively in Kelvin[4]

I.2.2 Conduction drying

Indirect drying is characterized by the transfer of heat through a conductive wall heated by a heat transfer fluid such as air, water, gas or water vapor. The heat transmitted by conduction causes the evaporation or vaporization of the liquid contained in the product. The vapor thus generated is then evacuated by a slight flow of auxiliary gas or by a vacuum effect. Heat transfer by conduction allows the diffusion of energy to the internal layers of the product, in accordance with Fourier's law. This mechanism ensures a progressive transmission of heat through the material, thus promoting the uniformity of the thermal process.[2]

$$\varphi_{cond} = -\lambda * S_p * \frac{dt_p}{dx} \text{ [4]} \quad \text{(I.2)}$$

I.2.3 Radiation drying

In this type of drying, the energy required for evaporation is provided by light radiation. This process is particularly effective in removing water, especially when the product concerned is not sensitive to heat. Radiation sources may include emitters operating on combustible gas, electrical devices or solar radiation. The quantity of heat Q, expressed in watts, depends on the characteristics of the source used.[2]

I.2.4 By dielectric loss:

Dielectric loss drying relies on electrical heating of insulating materials, also called dielectrics. When a non-conductive material is exposed to an electric field, its molecules undergo polarization. Each time the polarity of the electrodes is reversed, the orientation of the

molecular dipoles changes, generating heat inside the material. This phenomenon allows moisture to be removed more efficiently than conventional methods, while ensuring uniform drying.

I.2.5 By freeze-drying:

Freeze-drying is a dehydration process carried out at low temperatures, allowing the water present in a product to be eliminated by sublimation. This technique preserves the properties of the product while extending its shelf life, by significantly reducing the water content. It is commonly used in the pharmaceutical, food and biological fields to ensure better stability of the substances treated.[5]

I.3 Deferent methods of drying

I.3.1 Mechanical drying:

This involves the removal of liquid by purely mechanical means, such as pressing, centrifugation, compression, decantation or filtration.

I.3.2 Chemical drying:

This process is based on the use of dehydrating substances, such as calcium chloride, to extract water by osmosis.

I.3.3 Thermal drying:

This process is mainly based on a mass transfer, preceded by an “activation” of the water, made possible by the contribution of a certain quantity of energy by thermal transfer.
The two transfers are split into an external phase and an internal phase:

- Heat transfer inside the product, from the heat source to its surface.
- Internal heat transfer, from the surface to the core of the product.
- Internal mass transfer, from the core to the surface of the product.
- External mass transfer from the product surface to the external environment.[6]

I.4 AIR DRYING:

This traditional method, still in use today, consists of exposing the products to be dried in the open air. Although simple and inexpensive, it has the disadvantage of causing significant losses. A comparative table has been established to highlight the advantages and disadvantages of drying in the open air compared to drying in a dryer. In order to optimize these ancestral techniques, professionals have developed various prototypes of solar dryers, thus promoting artificial drying

Table I.1: Advantages and disadvantages of solar dryer drying and open air drying[7]

Drying under solar dryer	Air dry
Benefits: ∗ Reduced drying time ∗ Control of the desired final water content. ∗ Protection of the product against ultraviolet radiation. ∗ Control of the drying process. ∗ Free energy source. Disadvantages: ∗ Use of conventional energy (electricity, gas, wood, etc.) in the case of a hybrid system. ∗ Relatively high investment cost. ∗ Qualified personnel required.	Benefits: ∗ Simple and economical method. ∗ Does not require any specific equipment or skilled labor. ∗ Use of free and environmentally friendly solar energy. ∗ No additional energy consumption. Disadvantages: ∗ Long drying time, increasing the risk of mold. ∗ Possible deterioration of product quality due to solar radiation.

I.5 THE DIFFERENT TYPES OF SOLAR DRYER

Solar dryers rely on solar energy for heat and are influenced by sunlight availability. Therefore, they are most suitable for regions with abundant sunshine and low humidity levels.

- Higher drying temperatures result in faster moisture evaporation and lower final moisture levels.
- Additionally, solar dryers help safeguard products from rain, dust, dirt, insects, and potential losses caused by birds and animals.

A cabinet solar dryer typically consists of a wooden frame enclosed with transparent plastic. Alternatively, metal frames and glass covers can be used, though they increase cost and weight. The cabinet includes vents at the top and bottom to facilitate airflow. To enhance durability, the plastic cover should be UV-resistant. Inside, trays are lined with plastic mesh, as metal or wire mesh is not recommended due to potential reactions between food acids and metal.

A solar dryer is a closed system designed to protect food from external threats such as birds, animals, insects, dust, and unexpected rain. It utilizes solar thermal energy to dry food in a more hygienic and controlled environment.

The adoption of solar dryers in developing countries can help minimize crop losses and enhance the quality of dried products compared to traditional drying techniques like sun or shade drying. Solar drying methods are generally divided into four categories based on how energy is transferred to remove moisture: sun drying, direct solar drying, indirect solar drying, and mixed-mode drying.[8]

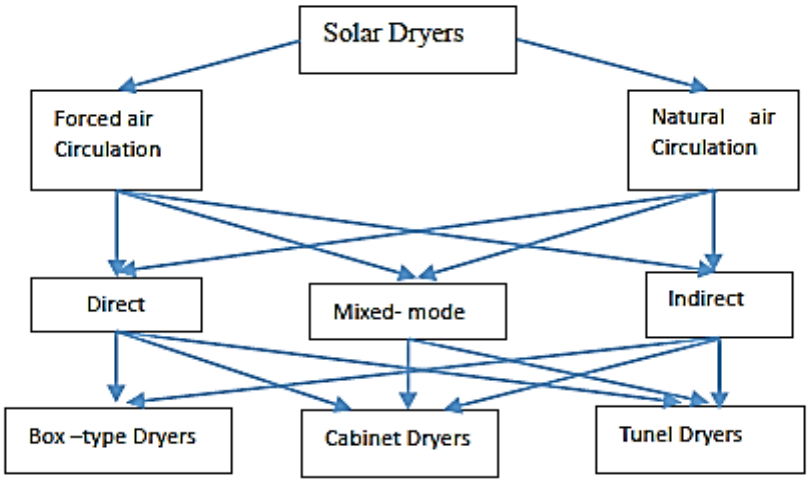

Figure I.1:Classification of solar dryers and drying modes [9]

I.5.1 Passive or natural air circulation:

Passive or natural air circulation relies on the use of solar energy to heat the air, increasing its capacity to absorb moisture from the products to be dried. The warm, lighter air rises naturally and escapes through a chimney, taking with it the extracted water vapour. This process works thanks to the chimney effect, without requiring any other energy source, making it particularly suitable for isolated areas without access to energy networks. However, a major drawback of this type of dryer is the risk of overheating of the products, often caused by poor air circulation in the system.[7]

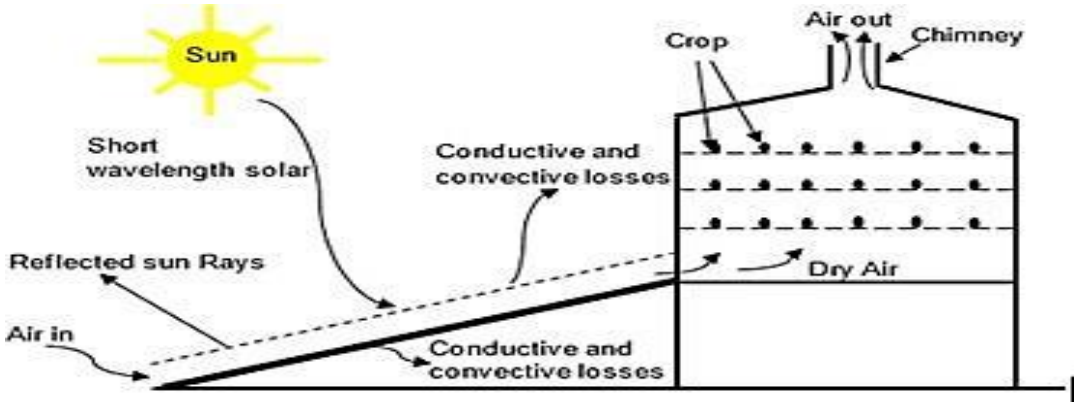

Figure I.2: illustrative diagram of a passive solar dryer [10]

I.5.2 Active solar or forced convection dryer:

In this type of drying, a fan is used to force the circulation of the drying fluid, thus improving the evaporation efficiency of the dryer. In general, forced convection offers much better performance than natural convection, which, despite advances in this field, does not yet allow precise control of the drying process.

This type of solar dryer offers better control of the drying process and allows reducing the drying time compared to passive dryers, thanks to a rapid and continuous evacuation of the air loaded with humidity. However, it has some disadvantages, including a higher manufacturing and investment cost than passive dryers. In addition, its operation requires a source of electrical energy, whether from the conventional network or from photovoltaic panels, to power the fan. [7]

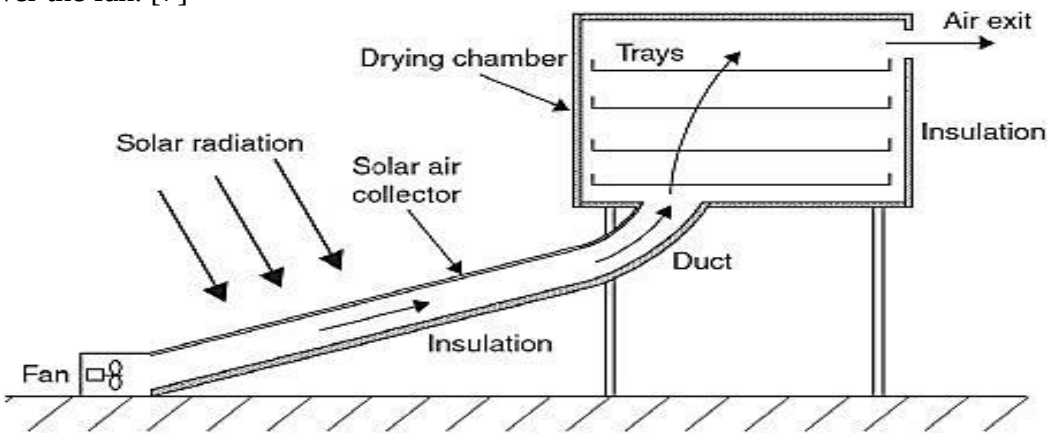

Figure I.3: Illustrative diagram of an active solar dryer [11]

I.5.3 Direct Solar Dryer:

In this type of dryer, the material is directly exposed to solar radiation within an enclosure covered with transparent glass or plastic. The sun's rays generate heat inside the enclosure through the greenhouse effect, raising the internal temperature above the ambient temperature. The transparent cover minimizes heat loss due to convection, further increasing

the chamber's temperature. To maximize heat absorption, both the collector and drying chamber are typically painted black. However, some heat is lost through convection and evaporation from the heated material.

Direct solar dryers are cost-effective and simple to operate but lack temperature control, making it challenging to protect the drying product from external elements. Sunlight penetrates porous materials, altering their color and texture. Prolonged exposure can lead to color changes in many fruits and vegetables and result in the loss of essential vitamins.[12]

Advantages:

- Cost-effective solution.
- Moderately fast drying process.
- Easy to build.
- Widely adopted technology.

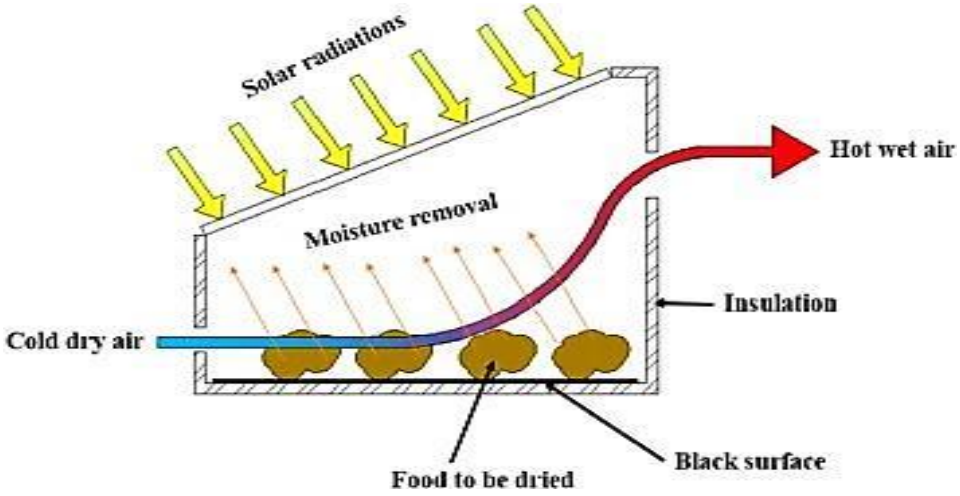

Figure I.4: Illustrative diagram of Direct Solar Dryer [13]

Disadvantages:

- Fragility of polyethylene materials requiring frequent replacement.
- Quite high internal temperature, combined with sun exposure, can alter nutrients.
- Insufficient air circulation, slowing drying and increasing the risk of mold.[3]

I.5.4 Indirect Solar Dryer:

In indirect solar dryers, the drying material is not directly exposed to sunlight. Instead, air is heated in a solar collector and then directed into a drying chamber, where it removes moisture from the product. This method allows for temperature regulation, resulting in higher-quality dried products compared to direct solar drying. Since the product is not exposed to ultraviolet radiation, its color and texture are better preserved. However, indirect dryers tend to be more costly to manufacture and require more complex operation.

Advantages:

- Preserves a high level of nutrients.
- Allows for precise temperature regulation.[12]

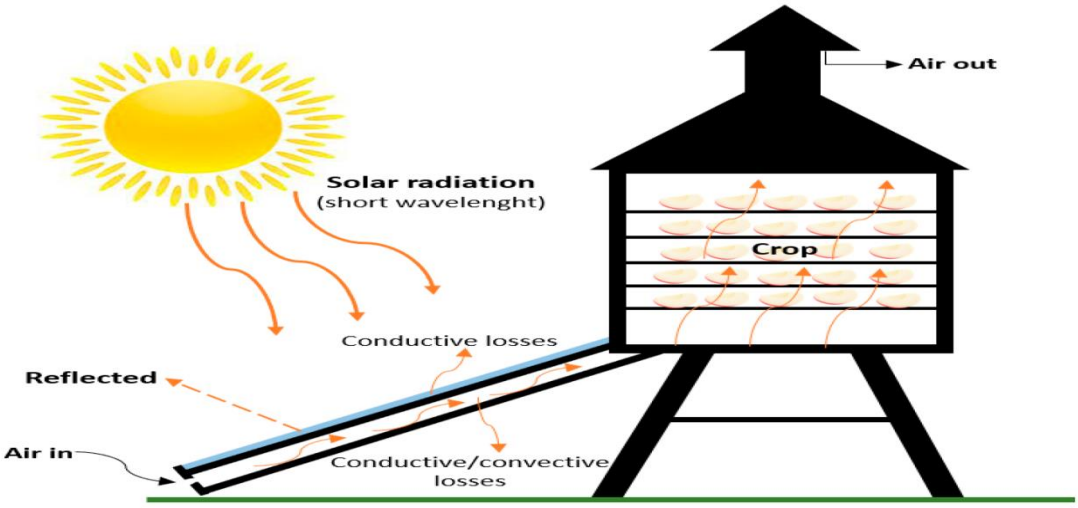

Figure I.5: Illustrative diagram of indirect Solar Dryer [14]

Disadvantages:

- Drying speed is highly dependent on climatic conditions and dryer design.
- Polyethylene materials are fragile and require frequent replacement.[3]

I.5.5 Mixed Solar Dryer:

In these dryers, both direct solar radiation on the material and preheated air from a separate solar collector work together to generate the heat needed for drying. The drying process occurs through a combination of radiation, which transfers heat downward, and convection, which circulates warm air from the solar air heater. This dual mechanism allows for faster drying compared to both direct and indirect solar dryers.[15]

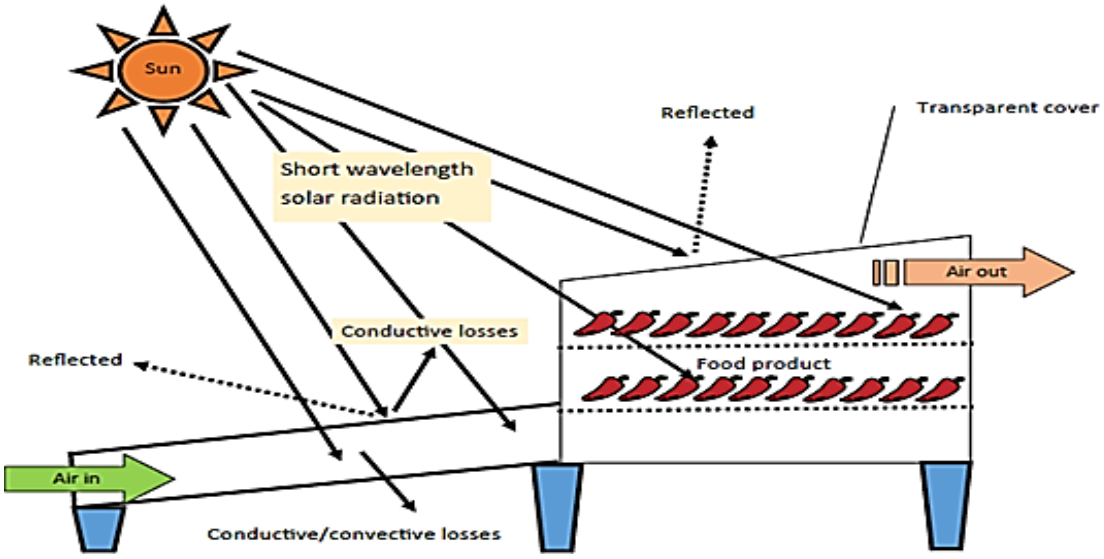

Figure I.6:Schematic of a mixed solar dryer [15]

I.5.6 Tunnel Solar Dryer:

A tunnel solar dryer is a long, high-capacity drying system designed to process large quantities of food efficiently. It operates similarly to a direct solar dryer but incorporates a fan powered by photovoltaic panels to enhance airflow and boost drying performance. This hybrid approach improves energy efficiency and enables continuous drying, even at night or during cloudy weather. While the initial investment is higher, tunnel dryers offer significant advantages, including reduced drying time, lower labor costs, and improved product quality.[12]

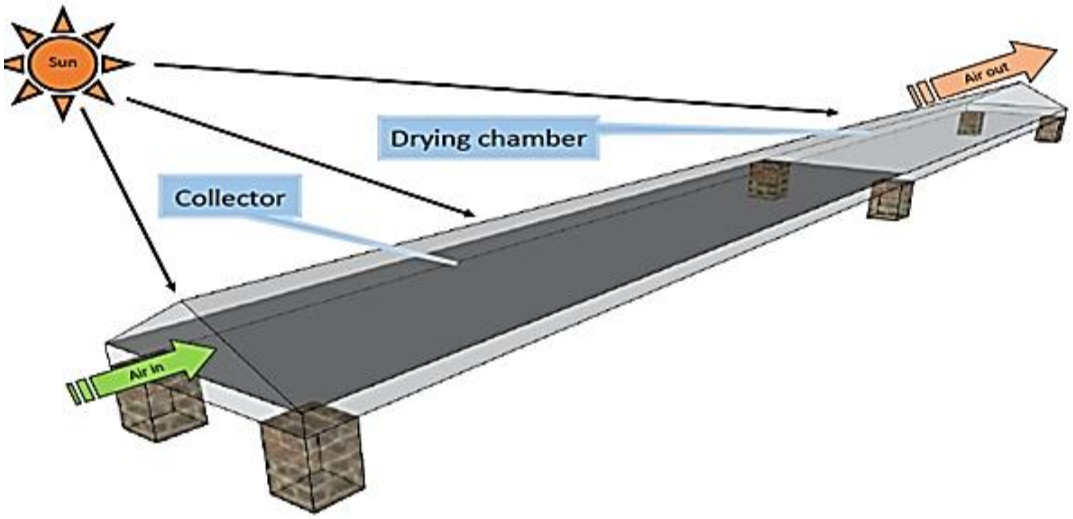

Figure I.7:Sketch and photo of tunnel solar dryer [12]

I.5.7 Hybrid solar dryers:

In this type of hybrid dryer, an auxiliary energy source (such as electricity, gas, fuel, wood, or biomass) is used to compensate for weather variations and regulate the drying air temperature through thermostatic controls. Hybrid solar dryers are more efficient than passive solar dryers as they can function even in cloudy conditions or at night. However, they come with certain drawbacks, including higher production and investment costs, dependency on local energy sources and spare parts, and the need for skilled personnel for maintenance.[16]

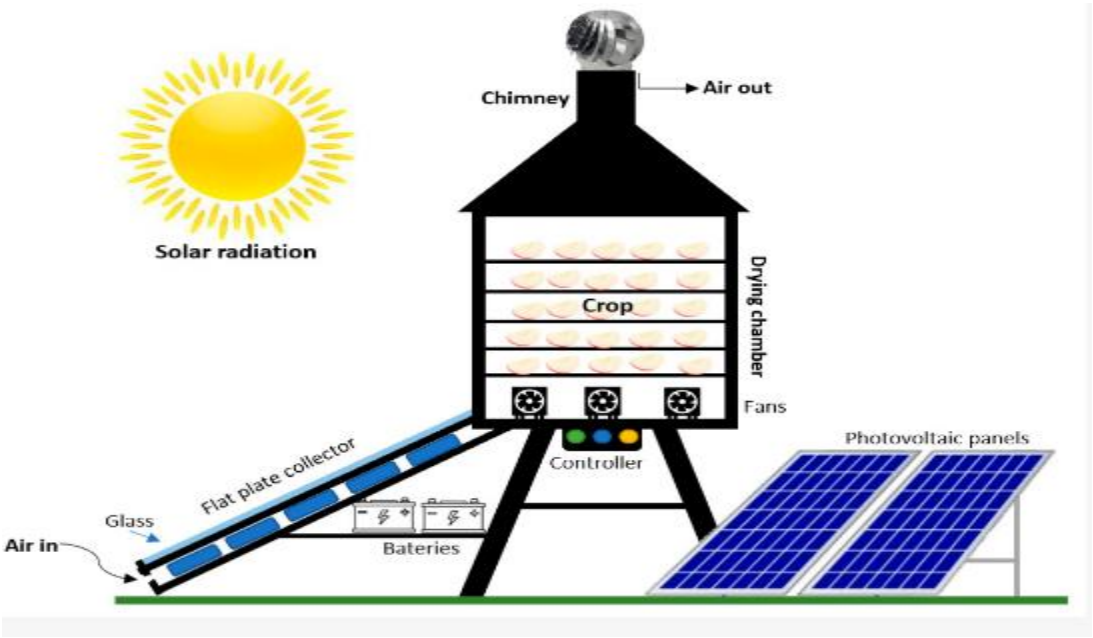

Figure I.8:Hybrid solar dryers [14]

I.6 Drying kinetics:

The study of the drying kinetics of various products is based on the analysis of curves illustrating the evolution of the drying speed as a function of time or the water content of the material (−dX/dT as a function of X). These curves are generally established under different experimental conditions, including temperature, drying air speed and hygrometry. They make it possible to characterize the overall behavior of the product during drying. The schematic curve presented in Figure (I.1) highlights three distinct phases of the process.

I.6.1 Transient early stage, (Period 0):

During this phase, the humidity of the product undergoes limited variations, while its temperature gradually changes (upwards or downwards) until it reaches the wet bulb temperature of the drying environment (zone A-B). This stage, generally brief, becomes more marked when the products have a large volume or when the temperature difference between the ambient air and the product is significant.

I.6.2 Period at constant speed:

During this phase, the drying rate remains relatively stable for most products. Moisture migrates to the surface in liquid form, mainly due to capillary forces. A balance is established between the diffusion of moisture through the boundary layer (located at the air-product interface) and the internal mechanisms of water transfer to the surface. The temperature of the material remains homogeneous, because all the thermal energy absorbed is used for the vaporization of water on the surface. This period, which represents a significant part of the

drying time, ends when capillary forces are no longer sufficient to maintain the evaporation of water on the surface.

The speed at which water is removed is directly linked to the rate of heat transfer, assuming the material's temperature remains constant. In this case, all the heat energy supplied contributes solely to the evaporation of water.

I.6.3 Falling rate period,:

At this stage, capillary forces are no longer able to transport water to the surface of the product. As a result, the drying speed can no longer remain stable and begins to gradually decrease

The falling rate phase can be separated into two distinct stages.

- First falling drying rate (C to D)
- Second falling drying rate (D to E)

- The initial stage of the falling drying rate happens as the wetted areas on the surface gradually shrink until the surface becomes completely dry (Point D).
- The second falling rate period starts at Point D, once the surface is fully dry, and continues until the equilibrium moisture content (EMC) is attained.[17]

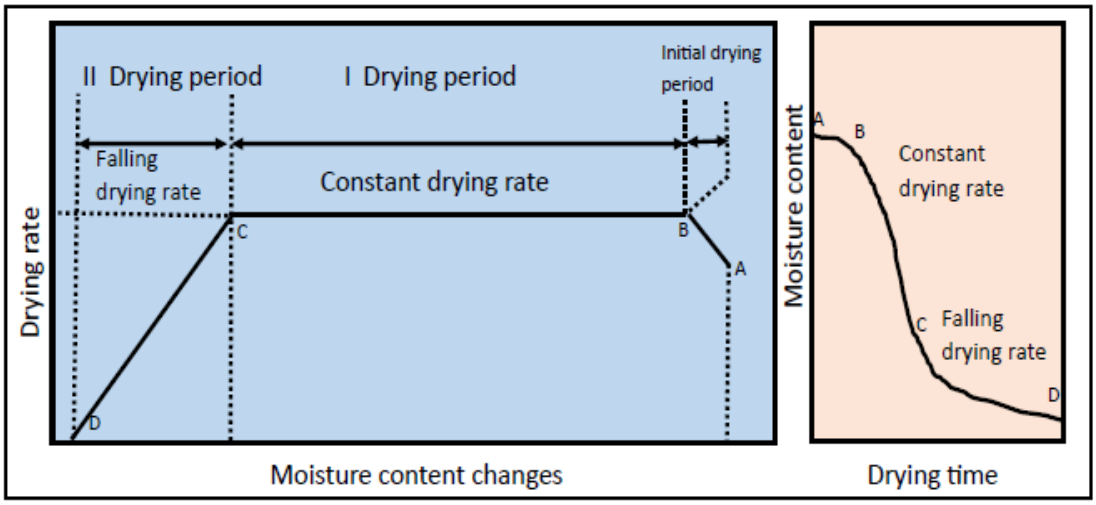

Figure I.9:Drying kinetics [8]

I.7Influence of air parameters on drying kinetics

I.7.1 Influence of air temperature:

The drying air temperature plays a key role in the drying speed. This influence is explained by the increase in heat input to the product as the air temperature rises. In addition, the product temperature increases in relation to the air temperature, which promotes faster diffusion of water inside the material.

I.7.2 Influence of air speed:

Air velocity promotes the drying process, especially in the early stages. However, for materials where internal water migration governs the drying kinetics, its impact becomes negligible.[3]

I.7.3 Influence of air humidity:

Air humidity significantly influences the drying kinetics of certain products. As with air speed, this effect is more pronounced at the beginning of the process and diminishes as the air temperature rises.[18]

I.8 Drying speed:

The drying rate corresponds to the rate of evaporation of the water contained in the solid to be dried, related to the unit of time and the mass of the dry solid. More precisely, it is defined as the limit of the quotient of the variation in water content (Δm) over the time interval (Δt). This quantity concretely reflects the dynamics of mass transfer during drying.

The drying speed depends on several factors, among which the most determining are:

- ✓ The nature, porosity, shape and humidity of the product.
- ✓ Temperature, humidity and air speed.

$$Vs = \frac{-dMv}{S_S.dt} = \frac{Ms\ .dx}{S_S.dt} \quad (I.3)$$

$$Mv = Ms\ .dx \quad (I.4)$$

$$dx = Xe - Xs \quad (I.5)$$

Mv: The mass of evaporated water.

Ms: The mass of dry product.

dX: The variation in water content of the product to be dried.

Ss: The drying surface

Xe: Water content of product at the inlet.

Xs: Water content of product at outlet. [5]

I.9 HUMID AIR:

Convection drying is the most commonly used method in the chemical industry. It consists of exposing the material to be dried to a flow of hot, slightly humid air or gas, which causes the water contained in the solid to evaporate. The air or gas then becomes charged with humidity while cooling.

Humid air is composed of a mixture of dry air and water vapor. The main quantities used to characterize it are defined below.

I.9.1 Absolute humidity (X):

Absolute humidity, also called specific humidity or moisture content of a gas, corresponds to the mass of water vapor contained in one kilogram of dry gas. It is noted X and is expressed using the following relationship:

$$\mathbf{X = \frac{M_a}{M_e}} \quad \text{(I.6)}$$

I.9.2 Relative humidity (φ):

Relative humidity (φ) is defined as the ratio between the partial pressure of water vapor present in the air (P_V) and the saturation pressure of this water vapor ($P_{S,\theta}$) at a given temperature θ.

$$\boldsymbol{\varphi = \frac{p_v}{P_s}} \qquad \mathbf{0 \geq \varphi \geq 100\ \%} \quad \text{(I.7)}$$

In practice, absolute humidity(X) is more commonly used than vapor pressure (P_V). Thus, we define the degree of saturation (Ψ) as the ratio of absolute humidity of air at a given temperature (X) and the corresponding saturation absolute humidity(X_S)at the same temperature.

$$\Psi = \frac{X}{X_S} \quad \text{(I.8)}$$

I.9.3 Dry temperature T and wet temperature T_H of the air:

The dry temperature of air or a gas corresponds to the measurement displayed by a thermal probe exposed directly to the flow of air or gas, without protection against humidity. The difference (T-T_H) represents the relative humidity of the air.

- When the air is saturated with water vapor (φ=100%), this difference is zero, indicating that no evaporation can occur.
- It increases with the gap [$(\theta) - P_V$], which is the main factor driving mass transfer.

I.9.4 Enthalpy of humid air:

The enthalpy, notedH, of one kilogram of dry air associated with Y kg of water vapor at a temperature θ ºC corresponds to the amount of heat required to heat this mixture, under constant pressure, to the reference temperature 0ºC to θºC. The reference states considered are liquid water and dry gas at θ°C

$$H = cp_a\theta + Y(L_v + cp_e\theta) \quad \text{(I.9)}$$

Where cp_a and cp_e are the specific heats of air and water in the gaseous state respectively and L_v the latent heat of vaporization of water at 0ºC.

I.10 CARACTERISTIQUES DES SOLIDES HUMIDES:

I.10.1 Absolute humidity

The absolute moisture of a solid, also called water content or moisture on a dry basis, is defined as the ratio between the mass of liquid present in the product and its mass of dry matter.

$$X = \frac{M_h - M_s}{M_s} \quad (I.10)$$

I.10.2 Relative humidity

The relative humidity of a solid, also called water content or water content on a wet basis, corresponds to the ratio between the mass of liquid contained in the product and its total mass, including water.[7]

$$\varphi = \frac{M_h - M_s}{M_h} \quad (I.11)$$

I.11 Evaluation of solar dryers

Evaluating a dryer is essential to analyze its technical performance, compare its efficiency with other models and provide valuable insights to manufacturers to optimize their designs. It also allows users to choose the dryer best suited to their needs.

Generally, there is no standardized method for evaluating dryers. Their performance is analyzed by measuring and comparing various specific parameters chosen according to the needs.

The main parameters considered when evaluating a dryer are:[19]

I.11.1.1 Physical characteristics of the dryer :

- Type, shape and size of the dryer
- Drying capacity/load density
- Surface area and number of drying trays (if applicable)
- Ease of loading and unloading of products

I.11.1.2 Thermal performance:

- Drying time and drying speed
- Temperature and humidity of drying air
- Flow of drying air
- Efficiency of the dryer

I.11.1.3 Quality of dried product:

- Organoleptic quality (color, flavor, taste, aroma, texture)

- Nutritional elements
- Rehydration capacity

I.12 Forms of water in food:

Water in a food can generally exist in three distinct states[20]:

I.12.1 Hydration water:

The water of hydration of a food can be present in two main forms. It can exist as a film adhering to the surface of the solid or be trapped in pores and interstitial spaces by capillary forces, which is called “free water”. Conversely, when it is strongly retained by interactions with the solid matrix or with other water molecules, it is called “bound water”.

I.12.2 Constitutional water :

The water of constitution is integrated into the molecular structure of the solid, as is the case in gels. Its extraction, partial or total, leads to dehydration which alters the very structure of the material. During drying, the objective is not to eliminate this water, because this would profoundly modify the properties of the product by affecting its original molecular structure.

I.12.3 Water vapor:

Water vapor in dry air is distributed in free spaces that are not completely occupied by liquid water.

I.13 Types of changes in the quality of the dried product:

- ✓ Biochemical changes due to temperature
- ✓ Loss of aromas
- ✓ Physical and mechanical modifications

I.14 Dried products

Table (I.2) lists a selection of dried products, specifying their essential characteristics: water content before and after drying (expressed on a dry basis), as well as the maximum temperature tolerated during drying. These products are classified into several categories: cereals, tubers, vegetables and fruits, in accordance with the FAO nomenclature. The cyanobacteriumSpirulina is assimilated to vegetables because of its high water content. The initial water content of the products varies considerably, ranging from 30% for certain cereals (corn, millet, rice, etc.) to 1900% for tomatoes. The sugar content also fluctuates, reaching 27% in the case of bananas. Various factors influence the behavior of products during drying, leading to phenomena such as browning (enzymatic or not), the formation of a crust or an alteration of the colour. These effects are generally linked to exposure to heat and solar

radiation. The thicknesses mentioned in Table (I.2) correspond to the average height of the product layer subjected to drying.[21]

Table I.2:Characteristics of dried products [21]

dried product	Initial water content (%)	Final water content (%)	Sugar content (g/100g)	Maximum drying temperature (°C)
corn	32 - 54%	14 - 18%	3,64	60
rice	32%	12%	0,13	50
sorgho, mil	27%	16%		60
potato	233 - 400%	11 – 16%	5,8 – 7,2	65
Manihot esculenta	163 - 233%	11 – 20%	3,9	65
pineapple	400 - 567%	14 - 11%	6,4 - 14	65
Banan	257 - 400%	14 - 18%	14,8 - 27	70
cabbage	400%	5%	2,8-3	60-65
carrot	233%	5%	6,7	75
tomato	1900%	8%	2,8 – 3,5	50-60
chili pepper, pepper	245 - 567%	5-15%	2,2 – 4,7	70

The performance of an indirect solar dryer is governed by a combination of external conditions, product features, and system design.

- **Climatic conditions** play a crucial role, as parameters such as solar irradiance, ambient temperature, humidity level, and air movement significantly influence the thermal energy available and the evaporation rate of moisture.
- **The nature of the product** being dried also matters. Factors like its initial water content, physical dimensions, internal structure, and material composition determine the speed and uniformity of moisture release during drying.
- **Dryer-specific and operational characteristics** are equally important. The configuration of the drying system—whether natural or forced convection, the quality of insulation, choice of construction materials, and the arrangement of trays—directly impact heat distribution, airflow, and overall drying effectiveness.

I.15 Previous works

In this study, **Nabnan and Namanwan [22]** investigated the efficiency of a home solar dryer that uses direct forced convection to dry bananas. The dryer was designed in a parabolic shape

and featured a flat collector covered with polycarbonate panels to minimize heat loss while maximizing solar radiation absorption. Between January and July 2019, five batches of bananas, each weighing 10 kg, were dried using this system. The results indicated that the air temperature used for drying inside the dryer ranged from 35°C to 60°C between 8:00 a.m. and 6:00 p.m. Over four days, the moisture content of bananas decreased from 72% (based on humidity) to 28%, while sun-dried samples reached only 40% moisture during the same period. The solar dryer significantly reduced drying time by 48% compared to natural sun drying. Additionally, the dried bananas maintained high quality in terms of flavor, color, and texture. The estimated payback period for the dryer is approximately 1.1 years.

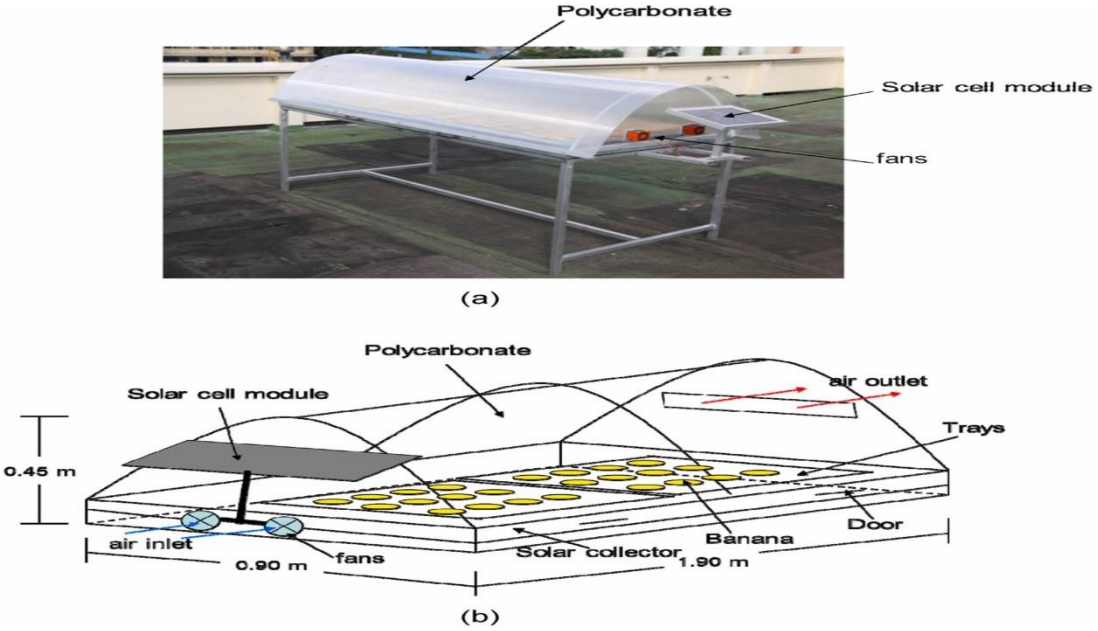

Figure I.10: (a) Pictorial view of the solar dryer and (b) schematic diagram of the solar drying system [22]

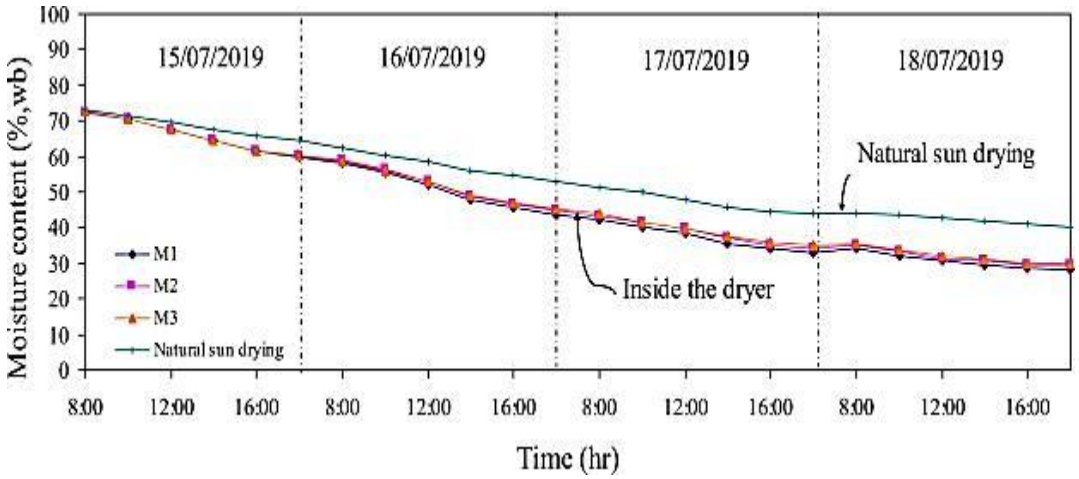

Figure I.11:Variations of air flow rate inside the dryer during a typical experimental drying run for banana [22]

Tefera and colleagues [23] analyzed the efficiency of two types of direct solar dryers for drying potatoes in Amhara Regional State: a wooden box model and a pyramid model. The objective of the study was to demonstrate their performance to local farmers by comparing them to traditional open-air drying. The parameters observed included temperature, relative humidity, and moisture removal rate, as measured by the weight loss of the potatoes. The results revealed a temperature difference of 10 to 20°C between the outside environment and the inside of the dryers. After two days, potato slices initially weighing 0.90 kg were reduced to about 0.19 kg, allowing a drying time saving of 2 to 3 hours compared to natural drying.Of the two models tested, the pyramid dryer proved to be more efficient, offering a more stable temperature and lower relative humidity. In addition, it was more economical and easier to build with local materials and accessible labor. Participants showed great interest in these new applications. The pyramid dryer, which is particularly suitable for drying small quantities of agricultural products (10-15 kg)**[23]**

Figure I.12: Box solar dryer [23]

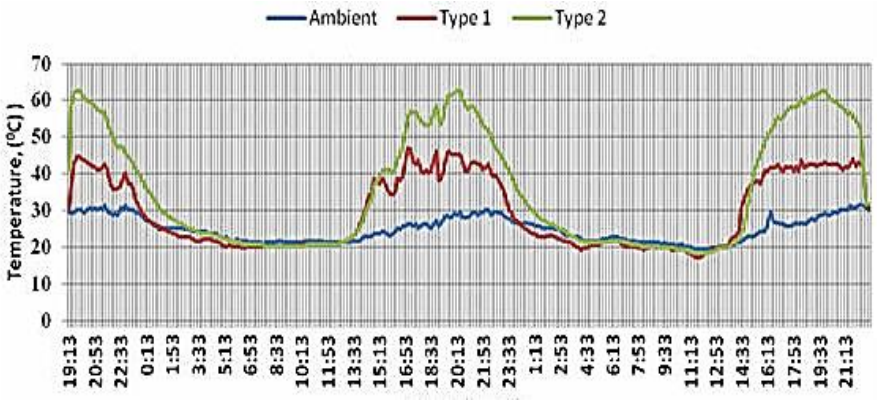

Figure I.13:Inside and outside temperature of solar dryers within trial periods [23]

JaouadEnnissioui, El MahjoubBenghoulam and Tarik El Rhafiki [24] studied the efficiency of an indirect solar dryer (ISD) specifically designed to adapt to the climatic and geographical conditions of Meknes, Morocco. This system includes a solar air collector (SAC) inclined at 34° to the ground, reaching a maximum outlet temperature of 58°C.During drying, banana slices experienced a significant mass reduction, from 549.76 g to 138.41 g.

The calculated average efficiency of the SAC was 23.37%, while that of the dryer reached 18.8%. Compared to open air solar drying (OSD), the ISD demonstrated a significantly superior performance in terms of moisture removal, reducing banana moisture by 74.83%, compared to only 39.08% for the OSD.The study also revealed that the moisture content of banana slices, initially 3.5771 kg/kg (dry basis), varied depending on the tray used, reaching 0.0397, 0.1292, 0.1745 and 0.2597 kg/kg (dry basis) for trays 1, 2, 3 and 4, respectively.

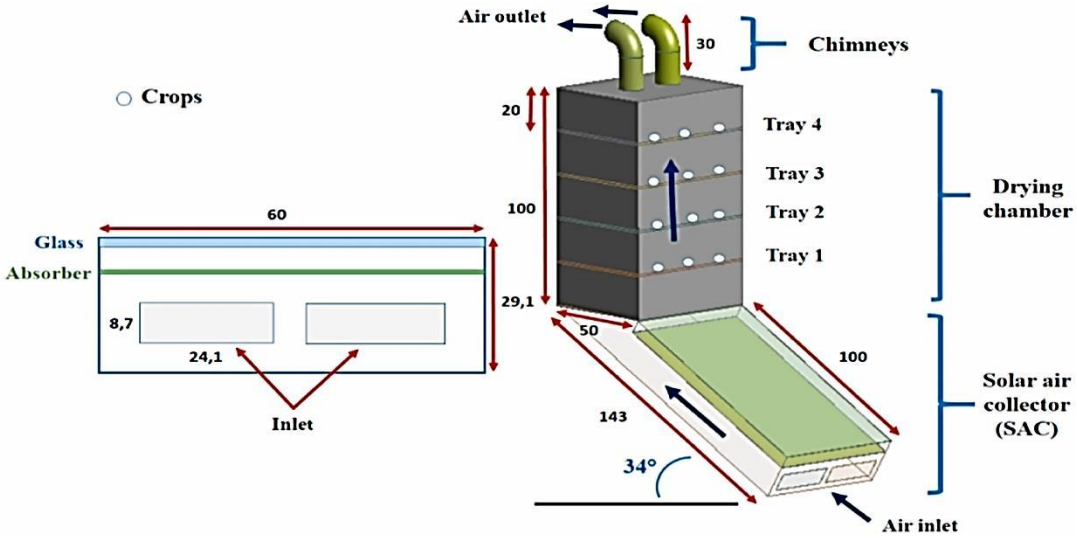

Figure I.14:Schematic representation of ISD and its elements [24]

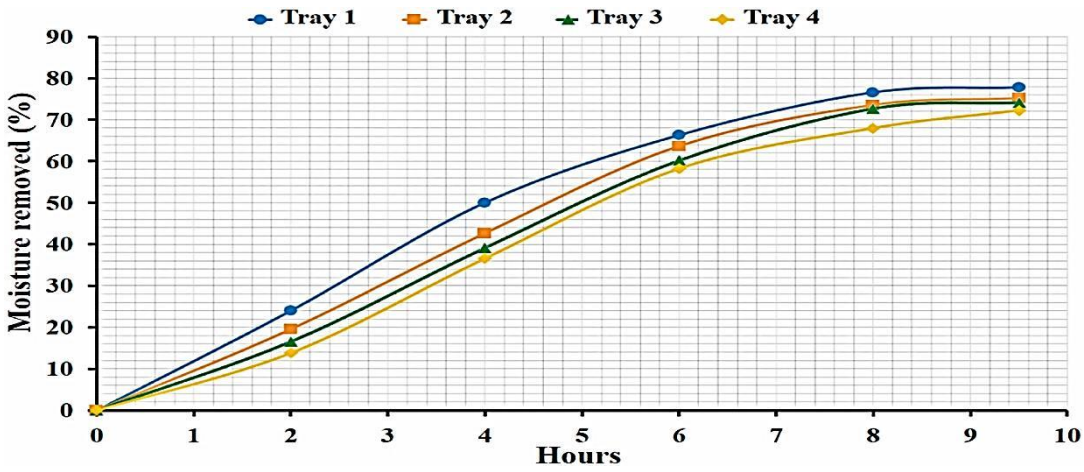

Figure I.15:Moisture removed from banana slices inside drying chamber vs. Time (h). [24]

The work carried out by **R. Slama [25]** and his collaborators concerns a solar dryer operating in indirect mode. Ambient air enters through the lower part of the collector and is heated using solar energy. The integration of baffles improves heat transfer, so that the air leaving the collector reaches a sufficiently high temperature. This hot air is then directed towards the drying chamber, where it transmits its heat to the product to be dried, thus promoting the evaporation of the moisture it contains. The air loaded with moisture is then evacuated to the outside by a forced ventilation system powered by a low-power electric fan.

The measurements carried out mainly concern the efficiency of the solar collectors taken individually as well as that of the dryer as a whole. In addition, the mass of the product is measured at the beginning and end of the process in order to evaluate the drying performance.

Figure I.16:Photograph of the indirect dryer [25]

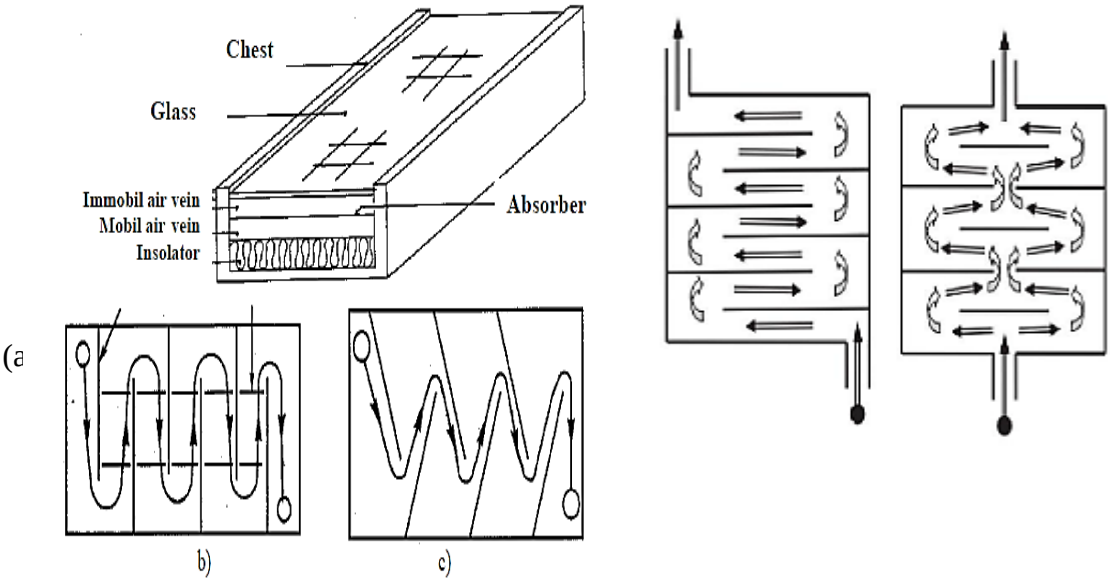

Figure I.17:Detail of the solar air collector showing: (a) its composition, (b) the straight baffles, (c) the oblique baffles, and (d) the flows generated. [25]

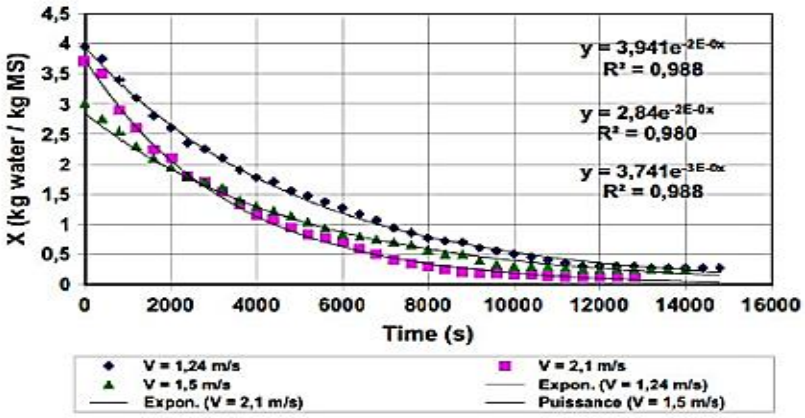

Figure I.18:Water content as a function of time and air velocity [25]

This work presented by **Shahrbanou Shamekhi-Amiri [26]** and his collaborators. This study aims to analyze the thin-film drying process of lemon balm leaves in a forced convection solar dryer operating in indirect mode. To optimize air heating, a solar air heater was used, associated with a double-pass packed bed equipped with a wire mesh structure. The experiments were performed on lemon balm leaves with an initial moisture content of 80% (wet basis) and were continued until reaching a residual moisture of 10%.

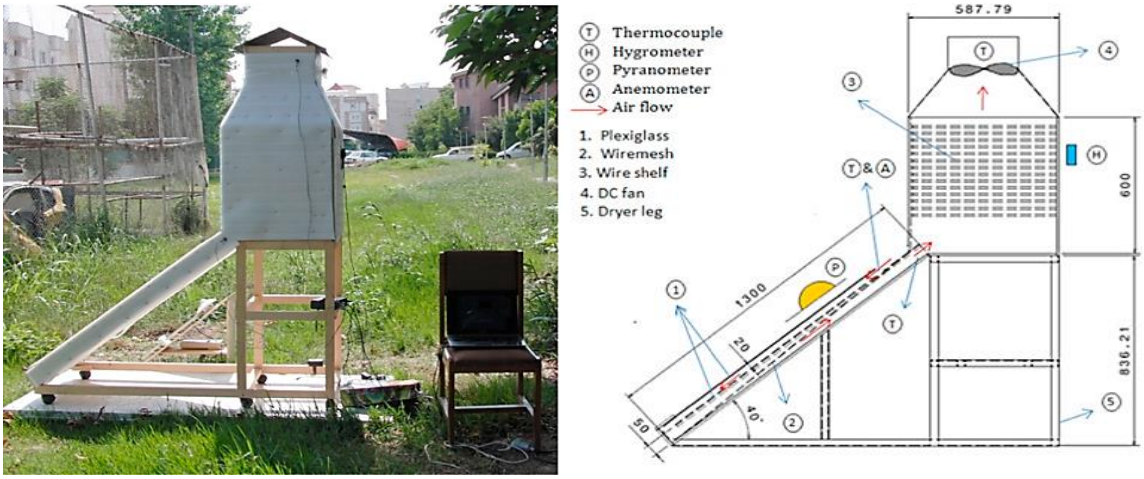

Figure I.19:Photos of the tested solar dryer [26]

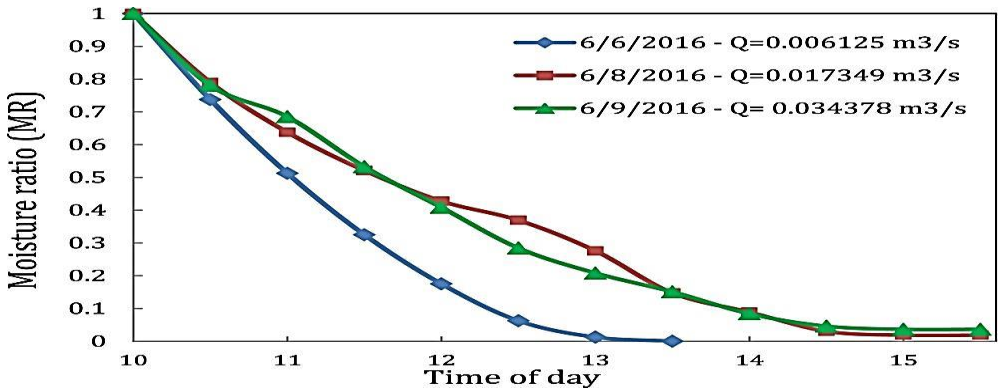

Figure I.20:Variation of moisture ratio versus drying time depicted at various airflow rates on different days [26]

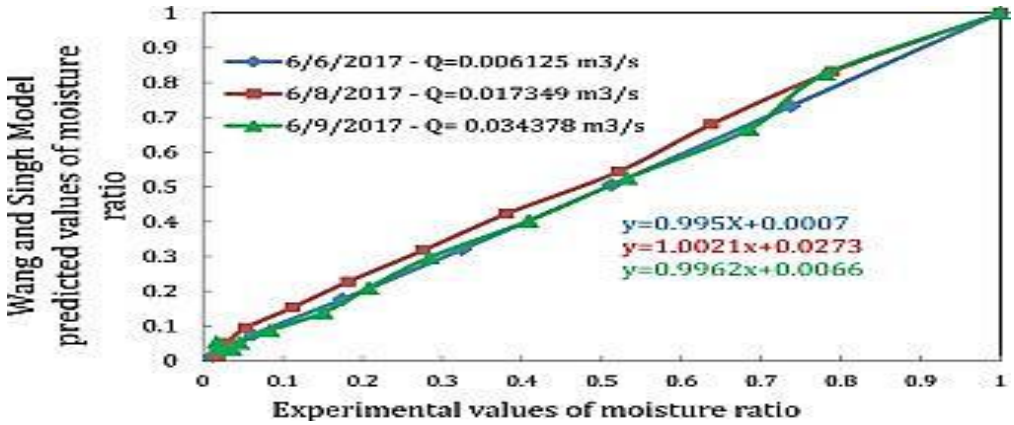

Figure I.21:Comparison between experimental moisture ratios and that predicted for lemon balm calculated using the Wang and Singh model. [26]

This work presented by **Nida Khan, K. Sudhakar and R. Mamat [27]** This research explores an innovative photovoltaic (PV)-integrated solar dryer developed to enhance the efficiency of seaweed drying by effectively reducing moisture content. Aimed at addressing the challenges faced by Malaysian seaweed farmers, the study compares traditional open sun drying with solar drying. Using 100-gram samples, experimental findings revealed that solar drying resulted in greater moisture loss, leading to significantly lower final weights for Sargassumpolycystum (43.8 g) and Cystoseirabarbata (40.1 g) compared to open sun drying (55.81 g and 52.9 g, respectively). Moreover, the drying rate in the solar dryer was higher, with Sargassumpolycystum reaching 7.03 g/hr and Cystoseirabarbata 7.5 g/hr, whereas open sun drying achieved 5.52 g/hr and 5.89 g/hr, respectively.

Figure I.22: photo and Graphical representation of solar dryer [27]

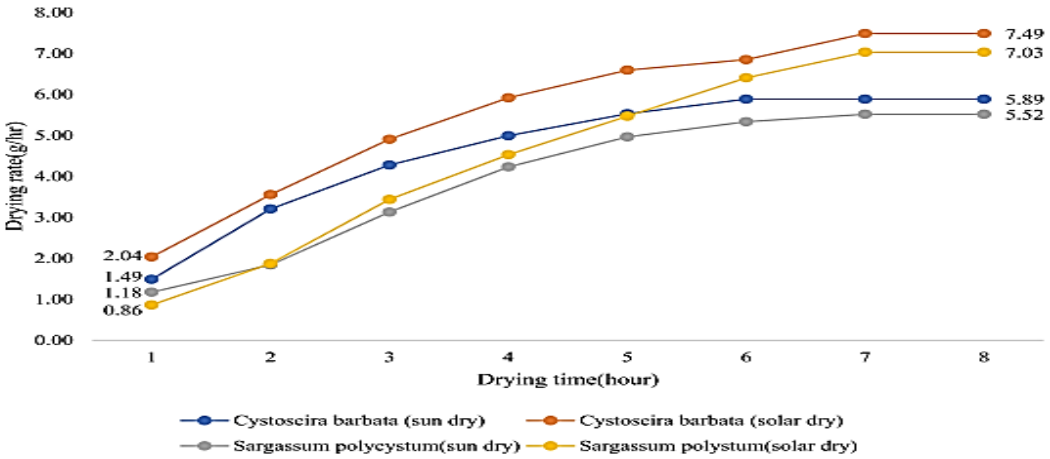

Figure I.23:Comparison of drying time vs drying rate. [27]

Jain and colleagues [28] conducted a study on the design and validation of a direct-type multi-shelf domestic solar dryer using computational fluid dynamics (CFD) simulation. Using ANSYS Fluent 14.0 software, they modeled and analyzed the operation of the dryer under

real-world conditions. The results showed that the internal air temperature reached 326 K, confirming the appropriateness of the designed model. The energy analysis revealed that the embodied energy of the building materials was 339.015 kWh, with an estimated energy payback time of 7.57. The convective heat transfer coefficient inside the dryer ranged from 2.4 to 2.8 W/m².K, indicating good thermal performance. In addition, the coefficient of determination, estimated at 0.98 under no-load conditions, demonstrated a strong agreement between the experimental results and the numerical predictions. This study highlights the interest of CFD simulations in the design and optimization of solar dryers, allowing to reduce costs and development time while ensuring increased efficiency of the device.

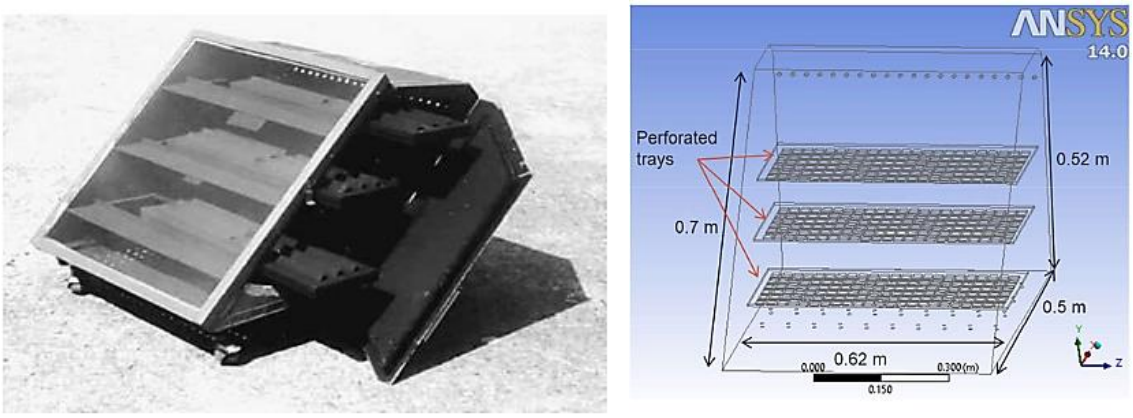

Figure I.24: photo and wire frame view of designed solar dryer [28]

Obayopo and his collaborators [29] developed an optimized direct solar dryer to improve fish preservation and reduce contamination risks. Given the limitations of traditional drying methods, they designed and numerically evaluated a specific model using computational fluid dynamics (CFD The study revealed that a 70×60×40 cm³ chamber with a tray placed 25 cm above the base allowed for homogeneous temperature and airflow distribution. The prototype, designed based on the simulation results, was experimentally tested in real conditions, during the dry and wet seasons, without load. The tests showed that the collector achieved a maximum efficiency of 77.2%, with a temperature increase of 26.7 °C in natural convection (without ventilation) in both seasons. Model validation was performed by comparing numerical predictions to experimental results using root mean square error (RMSE) and mean bias error (MBE), with deviations remaining within an acceptable margin of 10%. Statistical analysis via a t-test ($p \leq 0.05$) revealed no significant difference between observed and simulated values for all fan speeds tested.

This work demonstrates the contribution of CFD in the design of efficient solar dryers,

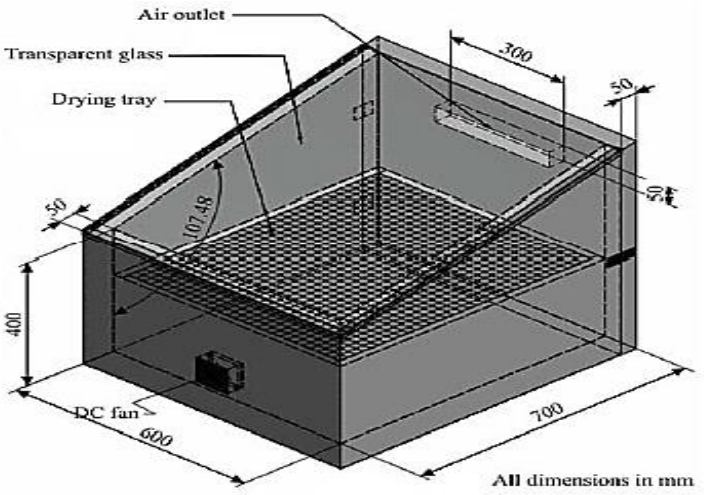

Figure I.25:Experimental Dryer [29]

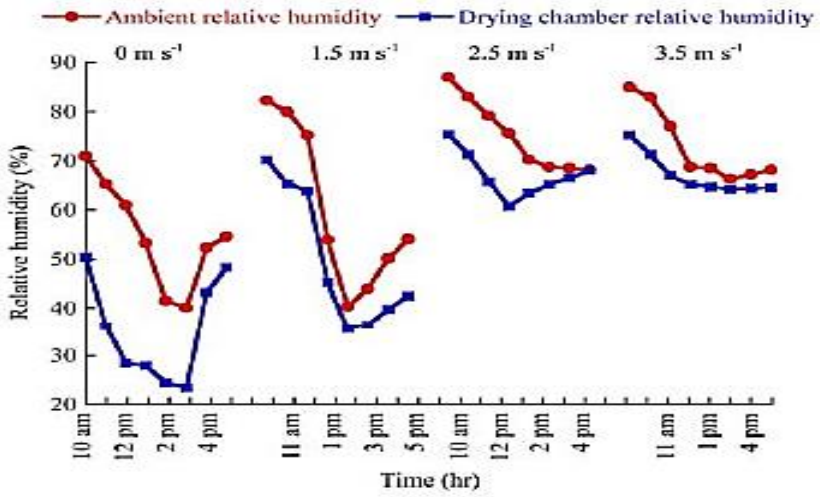

Figure I.26:Variation of humidity with relative time during the dry [29]

Ms. Chibot Romaisa [2] studied, realized and tested a solar dryer with natural and forced circulation implemented in the Department of Mechanics of the University of Blida 1 for drying food products indirectly. The air enters the sensor from the lower side or is heated along its path towards the exit at the upper part of the latter. The food, namely onions and tomatoes, was placed on three trays (stages) allowing the product to dry. The experimental results indicate that the evolution of drying temperatures is closely related to the variation of sunlight and ambient temperature. The drying time is shorter when the tests are carried out in a clear sky.

Figure I.27:Active or forced indirect solar dryer and drying chamber [2]

The following days were selected for testing the solar dryer:

05 and 12 and 14 and 18 et 19 juin 2023 will see the results of it :

Figure I.28: Fresh apricots before and after drying [2]

Afshari and colleagues [30] developed a compact and cost-effective solar dryer, tested with and without the addition of baffles. The study combined numerical and experimental analyses to evaluate the thermal performance and airflow inside the system. The results showed that both configurations performed well, but the addition of baffles significantly improved energy efficiency. Indeed, the average efficiency of the drying chambers was 44.91% for the dryer without baffles, compared to 55.28% for the one equipped with baffles, highlighting the positive impact of these elements on optimizing drying.

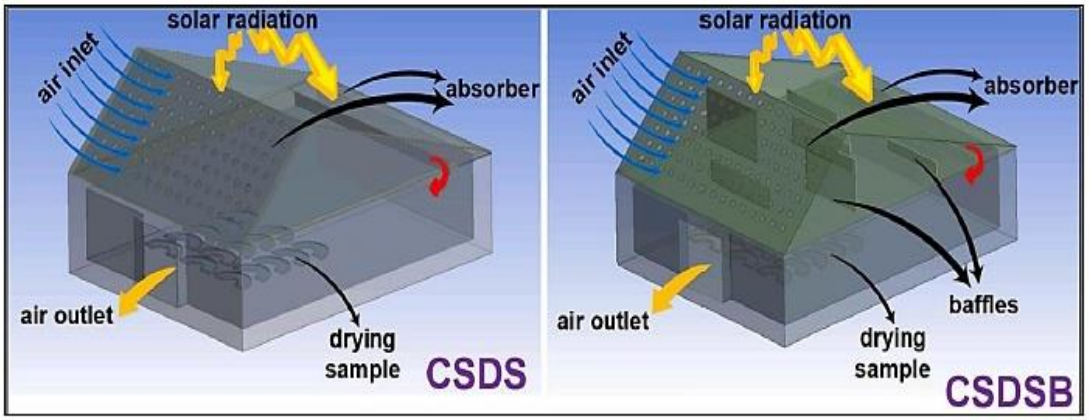

Figure I.29: Geometries and boundary conditions [30]

CONCLUSION :

Drying is a process that involves simultaneously a transfer of matter and a transfer of heat. It consists of extracting moisture from a solid by transforming the liquid it contains into vapor, which then dissipates in a gaseous medium. This transformation is made possible by an input of heat, which allows the change of state of the liquid. Vaporization can occur either by evaporation or by boiling, depending on the thermal and pressure conditions applied to the product.

Chapter II:

DETERMINATION OF SOLAR POSITION

II.Introduction

To design and optimize the performance of an indirect solar dryer, it is crucial to determine the sun's path and its positional variations—specifically the solar altitude angle (h) and azimuth angle (α)—throughout the day and across different seasons. This enables real-time simulation of the dryer's operation and accurate estimation of the actual solar radiation received. To achieve this, a MATLAB program was developed using astronomical equations to precisely track the sun's position and evaluate system performance. The simulation aims to calculate the solar elevation and incidence angles during the day and to identify the optimal drying periods based on solar availability.

II.1 Geographical location of the study

The city of Ghardaia, located in Algeria, was chosen as the study site due to its desert climate, which ensures a high level of solar radiation and sunshine throughout most of the year—ideal conditions for solar drying applications. Geographically, the city lies at a latitude of 32.8433° North and a longitude of 3.6667° East. To analyze solar position and radiation across different seasons, three representative days were selected: March 21st (the 80th day of the year) to represent the peak of spring, June 21st (the 172nd day) for the peak of summer, and December 21st (the 355th day) for the peak of winter. These parameters serve as the essential inputs for calculating the sun's position and evaluating solar energy availability at the selected location.

II.2 Sun Position Parameters

II.2.1 Solar declination δ:

Solar declination is the angle formed between the sun's rays and the plane of the Earth's equator. It varies throughout the year depending on the Earth's position in its orbit. Among the mathematical expressions used to calculate it, we find the one proposed by Cooper [31] , formulated as follows:

$$\delta = 23.45 \sin\left(\frac{360}{365}(N_J + 284)\right) \text{ (degree)} \qquad \text{(II.1)}$$

II.2.2 Hour angle ω:

The hour angle represents the apparent position of the sun relative to the local meridian, measured from solar noon. It is considered positive before solar noon and negative after. the sun appears to move 15° per hour. This angle can be determined using the following relationship:

$$\omega = 15(12 - TSV)\text{(degree)} \qquad \text{(II.2)}$$

TSV: True solar time expressed in hours.

II.2.3 Height of the sun h:

Solar altitude refers to the angle between the direction of the sun and the horizontal plane at the observation point. It is used to assess the sun's elevation in the sky at a given time. This angle can be calculated using the following expression:

$$\boldsymbol{sin(h) = cos(\varphi) . cos(\delta) . cos(\omega) + sin(\varphi) . sin(\delta)} \qquad \text{(II.3)}$$

φ:Latitude of the location.**ω:** Hour angle.

δ: Declination of the sun.

II.2.4 Universal Time (TU) :

Greenwich Mean Time (GMT) is the mean solar time measured along the reference meridian through Greenwich, which is considered the central meridian of the reference time zone. It serves as a universal time scale.

$$\mathbf{TU = TL - \Delta H} \qquad \text{(II.4)}$$

TL: Local solar time (from 6:00 AM to 20:00 PM) withtime difference between the Greenwich meridian and the state in question, in Algeria $\boldsymbol{\Delta H = 1}$

II.2.5 True solar time (TSV):

True solar time is the measurement of time based on the actual position of the Sun in the sky, reaching its maximum when it is at its highest point in the day (solar noon). This measurement fluctuates throughout the year due to two main factors: the tilt of the Earth's axis and the eccentricity of the Earth's orbit around the Sun. True solar time can be expressed by the following relationship:

$$\boldsymbol{TSV = TU + \frac{ET}{60} + \frac{\lambda}{15}} \qquad \text{(II.5)}$$

II.2.6 the equation of time:

it is the equation of time, it is expressed by the mathematical expression which is proposed by (Duffie and Beckman 2013).

$$\boldsymbol{ET = 9.87\, sin(2\beta_0) - 7.53\, cos(\beta_0) - 1.5\, sin(\beta_0)\ (Minute)} \qquad \text{(II.6)}$$

The angleβ_0 is defined based on the number of the day of the year:

$$\boldsymbol{\beta_0 = \frac{360}{365}(n_j - 81)} \qquad \text{(II.7)}$$

II.2.7 Azimut α :

The solar azimuth is defined as the angle formed between the horizontal projection of the direction of the sun and the southern axis of the observation location. It allows the position of the sun to be determined relative to the cardinal points, in addition to the solar height [31].

$$\alpha = \tan^{-1}\left(\frac{\sin(\omega)}{\cos(\omega).\sin(\varphi) - \tan(\delta).\cos\varphi}\right) \quad \text{(II.8)}$$

as the figure II.1 illustrates the two astronomical angles important for determining the sun's position in the sky: the elevation angle, which represents the sun's height above the horizon, and the azimuth angle, which determines the horizontal direction of the sun's position relative to the north. Understanding these two angles is essential for improving the design of solar systems such as solar dryers.

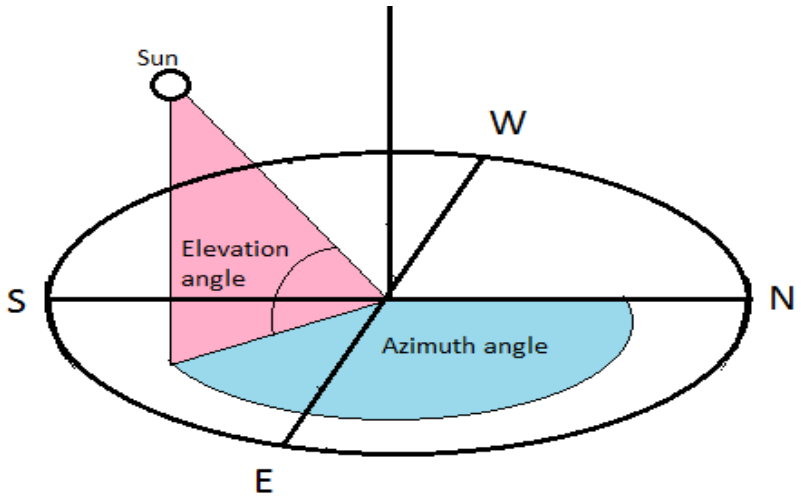

Figure II.1:Solar angles in determining the position of the sun[32]

II.3 The Results :

This section presents the calculated solar height and azimuth angles for three representative days of the year: 21st March (spring equinox), 21st June (summer solstice), and 21st December (winter solstice). These dates were specifically selected to represent key points in the solar calendar and to reflect seasonal variations in solar radiation. They are commonly used in solar energy studies to provide an overview of solar behavior throughout the year. In the context of this study, which focuses on the performance of a solar dryer, these days help assess the system's behavior under different solar conditions—moderate in spring, maximum in summer, and minimal in winter. The results include plots showing the sun's apparent trajectory across the sky on each day. The highest solar elevations occur around solar noon along the azimuthal path. On 21st June, the sun reaches its peak height and follows the

longest arc, providing the highest potential for solar energy capture. Conversely, on December 21st, the sun's path is shorter and lower, corresponding to reduced solar input. 21st March shows an intermediate trajectory. These variations are essential for evaluating the annual performance and orientation strategy of the solar dryer.

II.3.1 Sun position on March 21st :

Figure II.2 illustrates the daily variation of the solar azimuth angle (Az) on March 21st , a date close to the spring equinox. The horizontal axis represents the time of day from 6:00 AM to 8:00 PM, while the vertical axis shows the azimuth angle in degrees, ranging from +100° to -100°. In the morning, the azimuth starts around +90°, indicating that the sun rises in the east. In the afternoon, the azimuth becomes negative, reaching about -90° as the sun sets in the west.

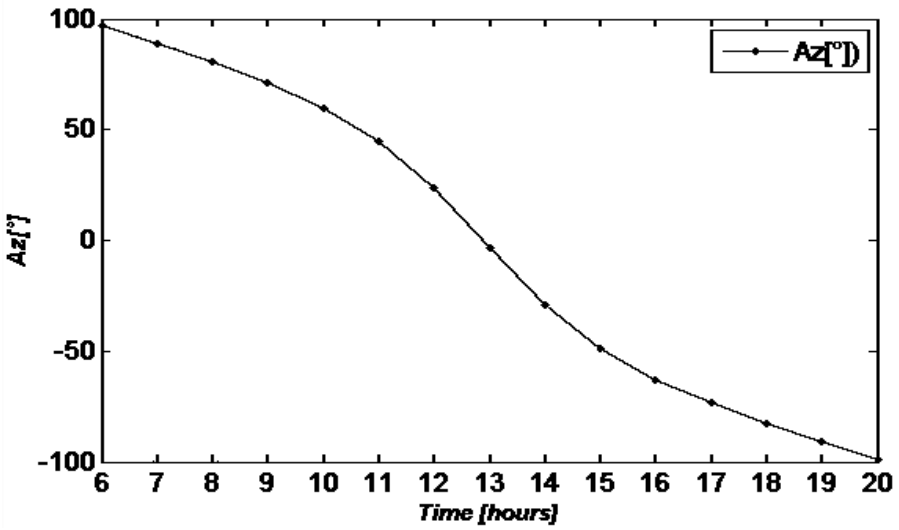

Figure II.2: Daily azimuth angle on March 21st

Figure II.3 presents the daily variation of the sun's height angle (also known as the solar altitude angle) on March 21st in Ghardaia, a date corresponding to the spring equinox. The x-axis represents the time of day from 6:00 AM to 8:00 PM, while the y-axis indicates the solar altitude in degrees. At sunrise, around 6:45 AM, the angle begins slightly below zero and rises steadily as the sun ascends in the sky, reaching its maximum value at solar noon (approximately 12:30 PM). It then decreases symmetrically as the sun moves toward the horizon, returning to zero at sunset, around 6:45 PM. This symmetrical, bell-shaped curve is characteristic of equinox days, during which day and night are nearly equal in length.

The variation of the sun's height angle throughout the day plays a crucial role in determining the intensity of solar radiation received on a given surface. This information is essential for optimizing the design, orientation, and operation of solar thermal systems, such as indirect solar dryers. On March 21st, the day length is approximately 12 hours, making it a

representative case for assessing solar system performance under balanced illumination conditions.

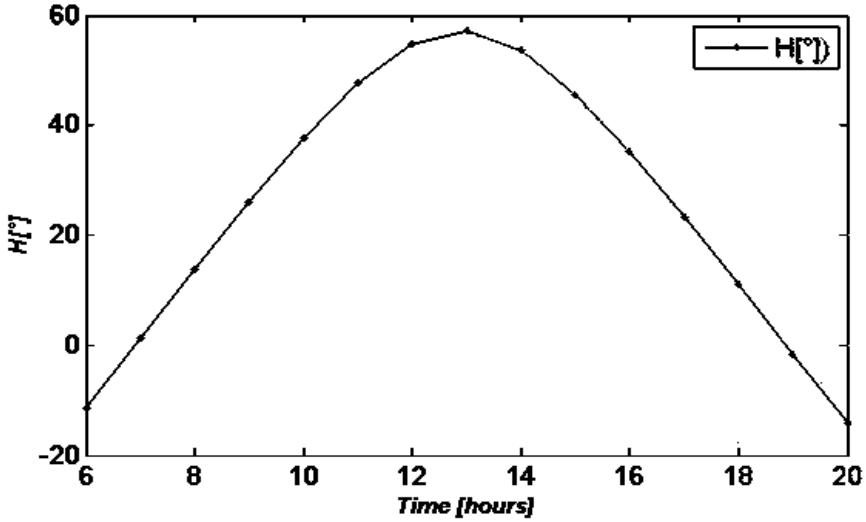

Figure II.3: Daily sun's height angle on March 21st

II.3.2 Sun position on June 21st :

Figure II.4 illustrates the daily variation of the solar azimuth angle on June 21st, the date of the summer solstice in Ghardaïa. The horizontal axis represents time from 6:00 AM to 8:00 PM, covering the full daylight period, while the vertical axis shows the azimuth angle in degrees, where 0° corresponds to true south. Positive values indicate directions east of south (morning), and negative values indicate directions west of south (afternoon). In the early morning, the azimuth angle starts around +115°, meaning the sun rises in the northeast. As the day progresses, the angle gradually decreases, reflecting the sun's movement across the sky from east to south. Around 1:00 PM, the azimuth angle approaches 0°, indicating that the sun is near true south and at its highest position in the sky, corresponding to solar noon and peak radiation. In the afternoon, the angle becomes negative, continuing to decrease to about -119°, showing that the sun moves toward the southwest and eventually sets in the northwest. This variation is crucial for analyzing solar exposure and optimizing the orientation of solar thermal systems like dryers.

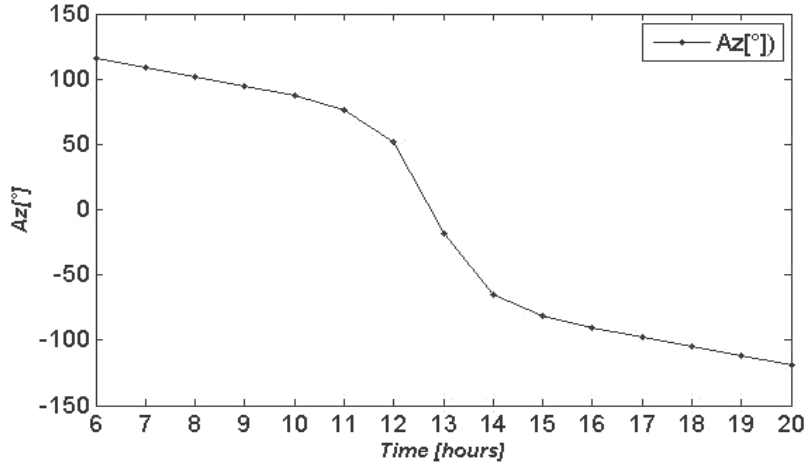

Figure II.4: Daily azimuth angle on june 21st

Figure II.5 shows the variation of solar height angle H with time on June 21st, the summer solstice. The sun rises at approximately 6:00 AM and sets at around 8:00 PM, resulting in about 14 hours of daylight. The solar altitude increases steadily from sunrise, reaching a maximum of about 80° at around 1:00 PM, which marks the solar noon, then symmetrically decreases until sunset.

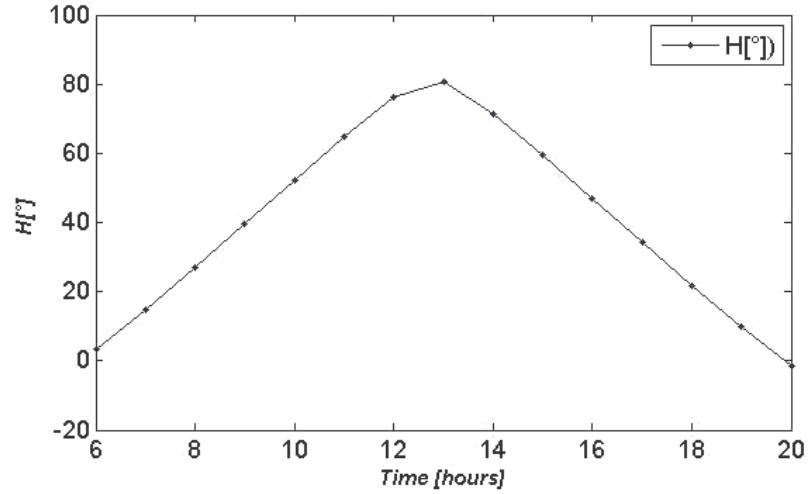

Figure II.5: Daily changes in the height of the sun in June 21st

II.3.3 Sun position on December 21st :

Figure II.6 shows the variation of the sun's azimuth angle throughout the day on December 21st, the winter solstice in the northern hemisphere. The azimuth angle starts at about **61.33° at sunrise** (southeast), increases gradually, and reaches around **-61.5° at sunset** (southwest). At **solar noon**, the sun's azimuth is close to **0°**, meaning it is due south. Compared to June 21st, the sun follows a shorter path across the sky, staying low on the horizon throughout the day.

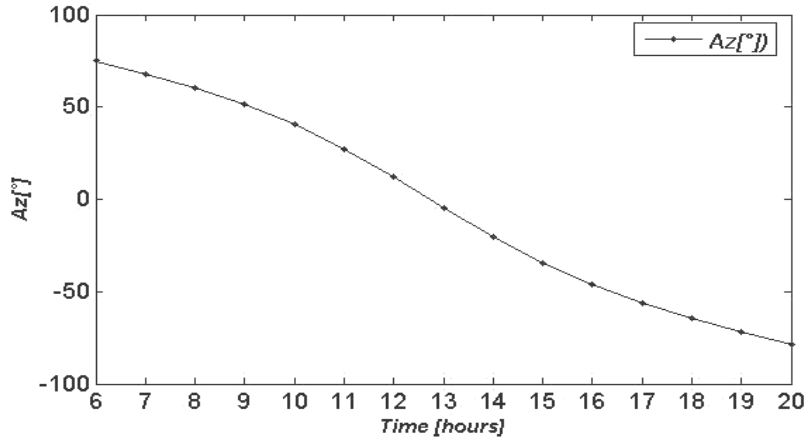

Figure II.6: Daily azimuth angle on December 21st

Figure II.7 illustrates variation the solar height angle with time on June 21st on December 21st, the winter solstice, showing a low and short arc from sunrise at 07:46 to sunset at 17:36. It depicts the sun rising in the southeast and setting in the southwest, with a limited daylight period of approximately 9 hours and 50 minutes. At solar noon, occurring at 12:43, the sun reaches its highest point in the sky, with an elevation angle of only 34.52°, which is clearly marked as the peak of the arc. This low solar trajectory reflects the minimal solar energy and long shadows typical of winter, emphasizing the shortest day and the lowest sun path of the year in the Northern Hemisphere.

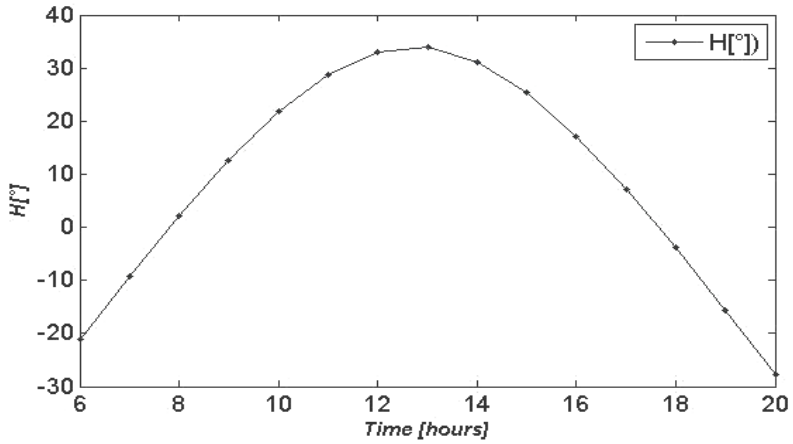

Figure II.7: Daily changes in the sun's height angle on December 21st

CONCLUSION :

Using a **MATLAB**, we simulated the sun's motion, a key factor in improving the performance of indirect solar dryers. It increases collector efficiency, improves hot air flow, shortens drying times, maintains the quality of dried products, and reduces reliance on conventional energy sources.

Chapter III:

Introduction to Solidworks and fluid flow simulation

III.Introduction

SolidWorks is one of the most powerful software programs used for 3D CAD design. Developed by Dassault Systèmes, it is widely used in various industrial and engineering fields, such as mechanical, aerospace, energy, and consumer products. The program combines design, analysis, simulation, and documentation tools in an integrated work environment, enabling engineers to accurately design parts and systems and analyze their performance before actual implementation.[33]

III.1 SolidWorks Overview

SolidWorks is a professional CAD (Computer-Aided Design) software developed for Windows, enabling engineers and designers to build detailed 3D models with an intuitive graphical interface. Its user-friendly approach streamlines the design process, making it easier to develop even complex geometries.

The software provides three primary workspaces tailored to different stages of product development:

- ✓ **Part Design**: Dedicated to creating and modifying individual 3D components with precision.
- ✓ **Assembly:** Allows users to combine multiple parts into functional mechanical systems, testing fit and motion.
- ✓ **Drawing:** Generates standardized 2D technical drawings directly from 3D models for manufacturing and documentation.

As The figure III.1 illustrates the design of an indirect solar dryer.

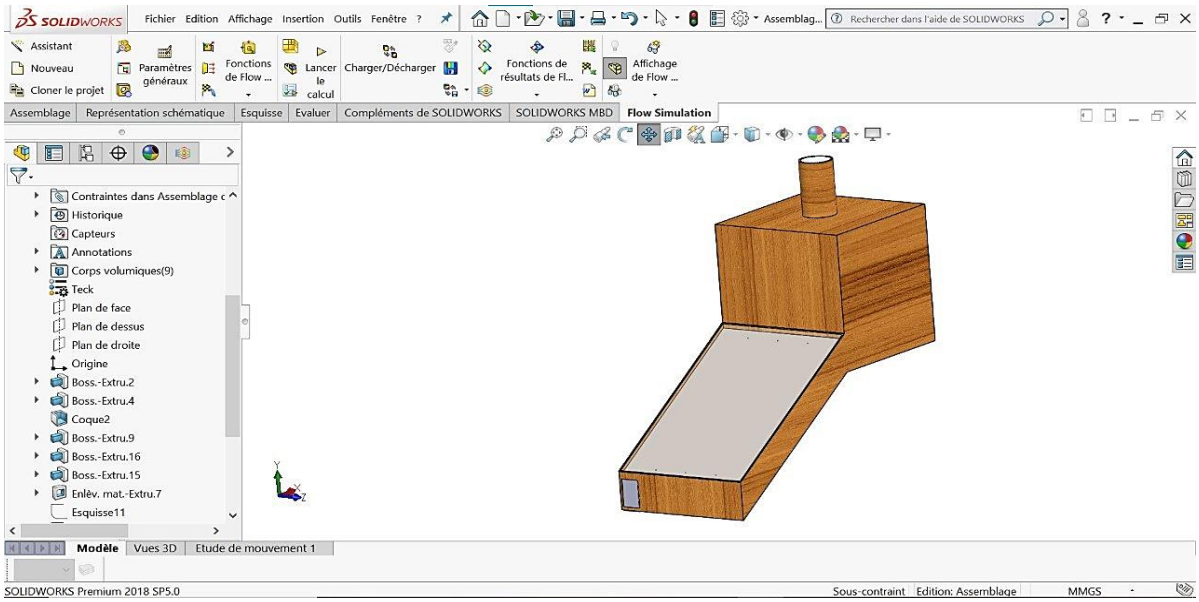

Figure III.1:Design of a solar dryer in SolidWorks

With these integrated environments, SolidWorks supports a seamless workflow from concept to production [34]

III.2 SolidWorks Advantages

SolidWorks stands out as a leading CAD software by combining powerful tools with user-friendly features. Here are some of its biggest advantages:

- ✓ **Intuitive and Easy to Learn :** With a streamlined interface, SolidWorks reduces the learning curve, allowing users to become productive faster than with many competing programs.
- ✓ **Seamless Design & Analysis Integration :** Perform simulations including structural, thermal, and motion analysis—directly within the software, eliminating the need for third-party tools.
- ✓ **Broad File Compatibility :** Import and export designs in universal formats like **STEP, IGES, STL**, and more, ensuring smooth collaboration across different platforms.
- ✓ **Extensive Standard Parts Library:** Access a vast built-in library of mechanical components, fasteners, and standard parts to speed up your design process.
- ✓ **Automated Documentation :** Generate technical drawings, bills of materials (BOM), and manufacturing documentation automatically, saving time and reducing errors.
- ✓ By combining efficiency, versatility, and industry-standard tools, SolidWorks helps engineers and designers bring their ideas to life faster and more accurately.

III.3 Uses of SolidWorks in Scientific Research

SolidWorks is a powerful tool for students and researchers, enabling cutting-edge academic projects at all levels—from undergraduate theses to PhD dissertations. Its advanced simulation and design capabilities support innovation across engineering and applied sciences.

Key Applications in Research and Education

- ✓ **Prototyping and Concept Development:** Design and refine functional prototypes of new devices, mechanical systems, or experimental setups before physical fabrication.
- ✓ **Performance Analysis and Optimization:** Conduct structural, thermal, and dynamic simulations to evaluate a model's behavior under real-world stresses, vibrations, or temperature changes.

- ✓ **Realistic Environmental Simulations:** Test designs under operational conditions, such as **fluid dynamics (CFD), heat transfer, or mechanical loading**, to validate theoretical models.
- ✓ **Iterative Design Enhancement:** Rapidly modify and improve designs using parametric studies, reducing development time and cost compared to physical testing.

By integrating simulation-driven design, SolidWorks empowers students and researchers to push boundaries, validate hypotheses, and contribute to technological advancements all within a virtual yet highly accurate environment.[35]

III.4 Case Study: Using SolidWorks in our Solar Dryer Design Project

As part of this study, SolidWorks was used as the core system for designing an indirect solar dryer. The software allowed for the design of the solar collectors, drying chamber, and air exchanger with high geometric accuracy. The following were also performed:

- Airflow analysis within the dryer using Flow Simulation tools.
- Temperature distribution in the dryer under the influence of solar radiation was studied.
- The impact of design on drying efficiency was evaluated.

This helped in making accurate design decisions before moving on to the practical implementation phase of the model.

III.4.1 Parameters used in Flow Simulation

Simulating the heat and air flow within a solar dryer using SolidWorks Flow Simulation relies on a set of basic parameters designed to represent real-world conditions as accurately as possible. These parameters include:

1. **air speed :**

The speed of the air moving within the dryer is a key factor in the drying process, directly affecting the rate of heat and moisture transfer. This speed can be generated by natural flow (due to temperature differences) or forced flow using a fan.

2. **Boundary conditions :**

It is used to specify how air interacts with model boundaries (such as inlets, outlets, and walls). The temperature and velocity of the incoming air, as well as the pressure at the outlet area, are determined. Walls can also be specified as either thermal insulators or as radiating or transferring elements.

3. Mesh :

Dividing the model into grids (or cells) is used to accurately calculate the heat distribution and air velocity. The grid resolution is chosen based on the complexity of the shape and areas where significant variations are expected, such as near vents or heated parts. This figure III.2 shows the flow simulation.

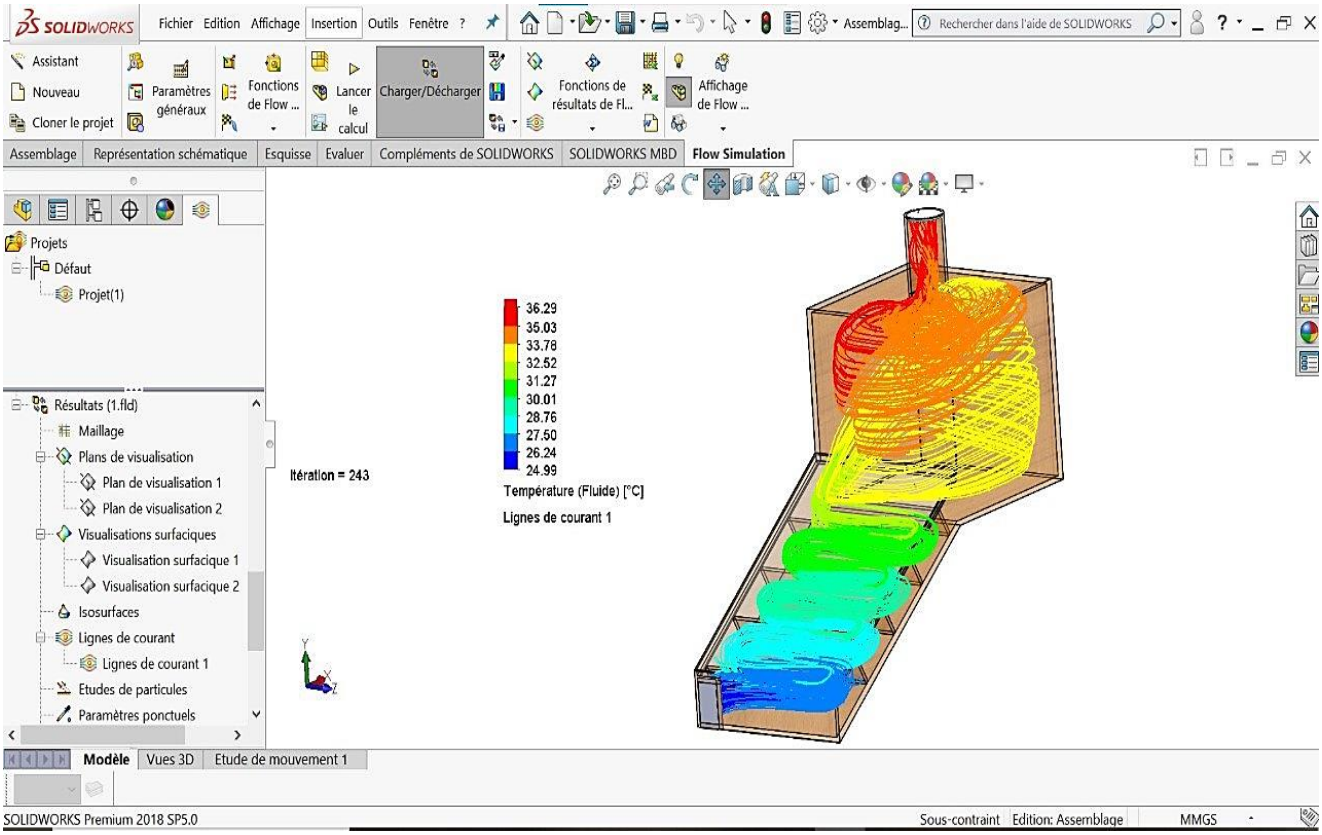

Figure III.2:Flow simulation of an indirect solar dryer

III.5 Mathematical Model:

The numerical analysis was performed using SOLIDWORKS software. This simulation relied on the application of the Navier-Stokes equations, which govern the principles of mass, momentum, and energy conservation in fluid dynamics.[36]

III.5.1 Continuity equation

This relationship guarantees that the amount of air entering and leaving the dryer remains balanced, maintaining mass conservation throughout the drying process.

$$\frac{\partial \rho}{\partial t} + \nabla.(\rho v) = 0 \qquad \text{(III.1)}$$

- ρ = fluid density (kg/m³)
- v = velocity vector (m/s)
- **t** = time (s)
- ∇= divergence operator

For an incompressible fluid, the density $\boldsymbol{\rho}$ is constant. Therefore:

$$\frac{\partial \rho}{\partial t} = 0 \qquad \text{(III.2)}$$

- $\boldsymbol{\rho}$ can be taken outside the divergence operator

$$\nabla.(\rho v) = \nabla \rho . v = 0 \qquad \text{(III.3)}$$

Since ρ is not zero, we divide both sides by ρ and obtain:

$$\nabla v = 0 \qquad \text{(III.4)}$$

Expand the divergence operator in Cartesian coordinates:

$$\frac{\partial u}{\partial x} + \frac{\partial v}{\partial y} + \frac{\partial w}{\partial z} = 0 \qquad \text{(III.5)}$$

III.5.2 Equation of motion

These equations express the balance of forces acting on each fluid component (such as air), including:

- Inertial forces (momentum),
- Pressure forces,
- Air viscosity forces.

In the x-direction:

$$\rho\left(u\frac{\partial u}{\partial x} + v\frac{\partial u}{\partial x} + w\frac{\partial u}{\partial x}\right) = -\frac{\partial p}{\partial x} + \mu\left(\frac{\partial^2 u}{\partial x^2} + \frac{\partial^2 u}{\partial y^2} + \frac{\partial^2 u}{\partial z^2}\right) \qquad \text{(III.6)}$$

In the y-direction:

$$\rho\left(u\frac{\partial v}{\partial y} + v\frac{\partial v}{\partial y} + w\frac{\partial v}{\partial y}\right) = -\frac{\partial p}{\partial y} + \mu\left(\frac{\partial^2 v}{\partial x^2} + \frac{\partial^2 v}{\partial y^2} + \frac{\partial^2 v}{\partial z^2}\right) \qquad \text{(III.7)}$$

In the z-direction:

$$\rho\left(u\frac{\partial w}{\partial z} + v\frac{\partial w}{\partial z} + w\frac{\partial w}{\partial z}\right) = -\frac{\partial p}{\partial z} + \mu\left(\frac{\partial^2 w}{\partial x^2} + \frac{\partial^2 w}{\partial y^2} + \frac{\partial^2 w}{\partial z^2}\right) \qquad \text{(III.8)}$$

$\boldsymbol{\rho}$: density.

u, v, w: components of air velocity in x, y, z directions.

$\boldsymbol{p}$: pressure.

μ**:** air viscosity.

III.5.3 Energy equation

This equation represents the transfer of thermal energy within a fluid (air in our case) as a result of both convection and conduction.

$$\left(u\frac{\partial T}{\partial x} + v\frac{\partial T}{\partial y} + w\frac{\partial T}{\partial z}\right) = \alpha\left(\frac{\partial^2 T}{\partial x^2} + \frac{\partial^2 T}{\partial y^2} + \frac{\partial^2 T}{\partial z^2}\right) \qquad \text{(III.9)}$$

T: Temperature.

u, v, w: components of air velocity in x, y, z directions.

$\boldsymbol{\alpha}$**:** Thermal diffusivity, which represents the fluid's ability to diffuse heat.

CONCLUSION :

SolidWorks has proven its effectiveness as a comprehensive tool for designing and analyzing engineering models. Its combination of 3D design features with simulation and analysis tools makes it an ideal choice for engineers and researchers. In the context of this project, SolidWorks was instrumental in building the digital model of the solar dryer and analyzing its performance, reducing time and cost and improving the quality of the final design.

Chapter IV :

NUMERICAL SIMULATION OF AIRFLOW IN THE SOLAR DRYER

IV. Introduction :

Algeria, blessed with abundant sunshine, offers considerable potential for harnessing solar energy, particularly in the preservation of agricultural products. Solar drying, in particular, presents an effective and sustainable solution for extending the shelf life of foodstuffs without resorting to conventional energy sources.

This chapter details the design and construction of an indirect solar drying system, adapted to the climatic conditions of southern Algeria. The system consists primarily of an air-source solar collector and a drying chamber, designed to maximize the efficiency of the dehydration process.

IV.1 Prototype of indirect solar dryer:

The objective of this current project is to design an indirect solar dryer for agricultural use, specifically for drying fruits and vegetables. The dryer is designed using SolidWorks software. The dryer consists of a 1-cubic-meter parallelepiped box. It is supplied with hot air via a flat solar collector inclined at an angle equal to the site's latitude (Ghardaia) of 32 degrees. as shown in the figure IV.1

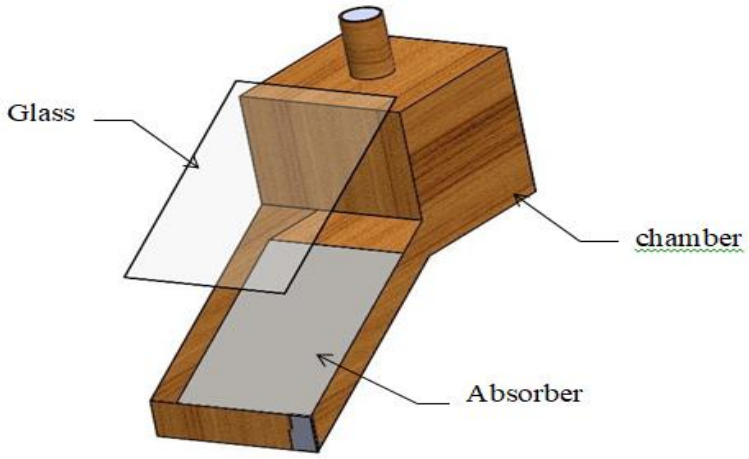

Figure IV.1:indirect solar dryer model

IV.1.1 System Description :

The prototype is an indirect solar dryer operating with forced and natural convection (ventilation) where the ventilation area and the air intake to the solar collector are equal (S = 314 cm^2). It consists of two modules: a drying box and a flat solar collector with air and a single glass. The collector has a parallelepiped configuration (1 m × 1.5 m), thus converting solar radiation into thermal energy transmitted by the air. The absorber is made of black-painted polished steel. It is also covered with 3 mm thick glass. Air flows between the two

planes of the absorber plate and the glass. To test this system, The simulation conditions are limited:

- absorbor temperature:70 °C
- fan speed: 2m/s
- Environmental pressure at the solar collector inlet

IV.1.2 Simulation results analysis :

The figure IV.2 represent the simulation results of the prototype indirect solar dryer in terms of temperature

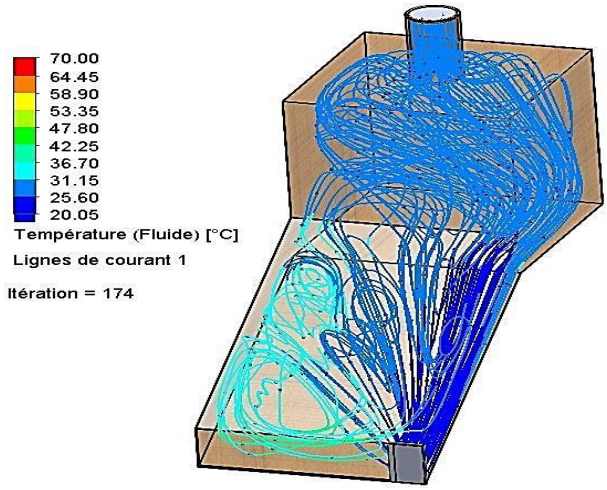

Figure IV.2:Simulation results of the indirect solar dryer model of temperature

The colors shown in the figure show a gradual distribution of temperatures , with red representing the highest temperature (~70°C) and blue representing the lowest temperature (~20°C). We note that the highest temperatures are concentrated at the top of the dryer near the outlet, reaching 28°C, indicating the accumulation of hot air due to convection.

The sky-blue streamlines indicate the airflow path within the dryer. The spiral movement of the air demonstrates that the dryer relies on natural convection, with hot air rising upwards and fresh air entering from below to compensate for the loss. We can see that air enters the solar collector at a temperature of 20°C and reaches the drying room at the same temperature. The spiral movement of the air demonstrates that the dryer relies on natural convection, with hot air rising upwards to reach 28°C in the center of the room and fresh air entering from below to compensate for the loss.

We notice irregular air movement on the right side of the solar collector, which is a result of uneven heat distribution and irregular flow.

The figure IV.3 represent the simulation results of the prototype indirect solar dryer in terms of air speed

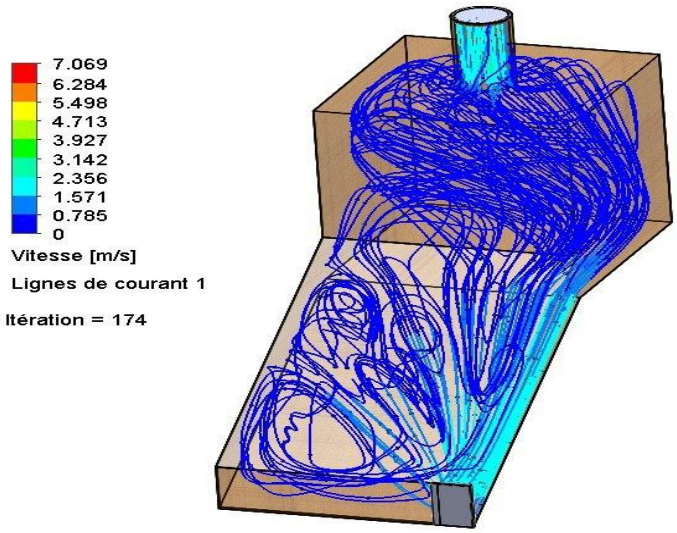

Figure IV.3:Simulation results of the indirect solar dryer model of air speed

The colors shown in the figure show a gradual distribution of air velocity, with red representing the highest velocity (~7.069 m/s) and blue indicating lower velocities (~0 m/s). We note that the highest air velocity increases at the lower inlet, reaching a speed of ~1.7 m/s, and at the top of the dryer near the outlet, reaching a speed of ~2 m/s, via ventilation, indicating a continuity of natural convection.

The sky-blue streamlines indicate the airflow path within the dryer. We observe vortices in the dryer's solar collector, indicating the presence of air recirculation zones. These vortices can affect heat distribution in an uneven manner, negatively impacting thermal uniformity and slowing the drying process. This necessitates improved ventilation or modified air paths to achieve more efficient drying. The upper part of the drying chamber indicates effective expulsion of moisture-laden air.

a) Design disadvantages :

- Temperature variations lead to inconsistent drying of materials.
- Some lower and side corners exhibit cool colors, indicating poor heat transfer. These areas impede the drying process and increase the duration of the process, reducing system efficiency.
- Air vortices in the heat exchanger cause air to be recirculated without effective upward movement, reducing drying efficiency.

Through our study of the initial design, we noticed some problems in the solar collector, so we made improvements to increase the efficiency of the indirect solar dryer, and this is what we will address in the new design.

IV.2 Improved model of indirect solar dryer:

The design of this improved model is inspired by design of Ms. ChibotRomaisa [2] with a change in ideas. .The improved model is an indirect solar dryer operating with forced and natural convection (ventilation), where the ventilation area and air inlet to the solar collector are equal (S = 314 m²). It consists of two modules: a drying box and a flat solar collector with air supply and a single pane of glass. The collector has a parallelepiped design (1 m x 1.5 m) consisting of air barriers spaced 15 cm apart. The absorber is made of black-painted polished steel with channels that allow hot air to pass through the channels and avoid thermal stress. It is also covered with 3 mm-thick glass spaced 3 cm apart. Air flows between the absorber plate and the lower part of the collector. as shown in The figure IV.4 We tested this system under the same simulation conditions as before :

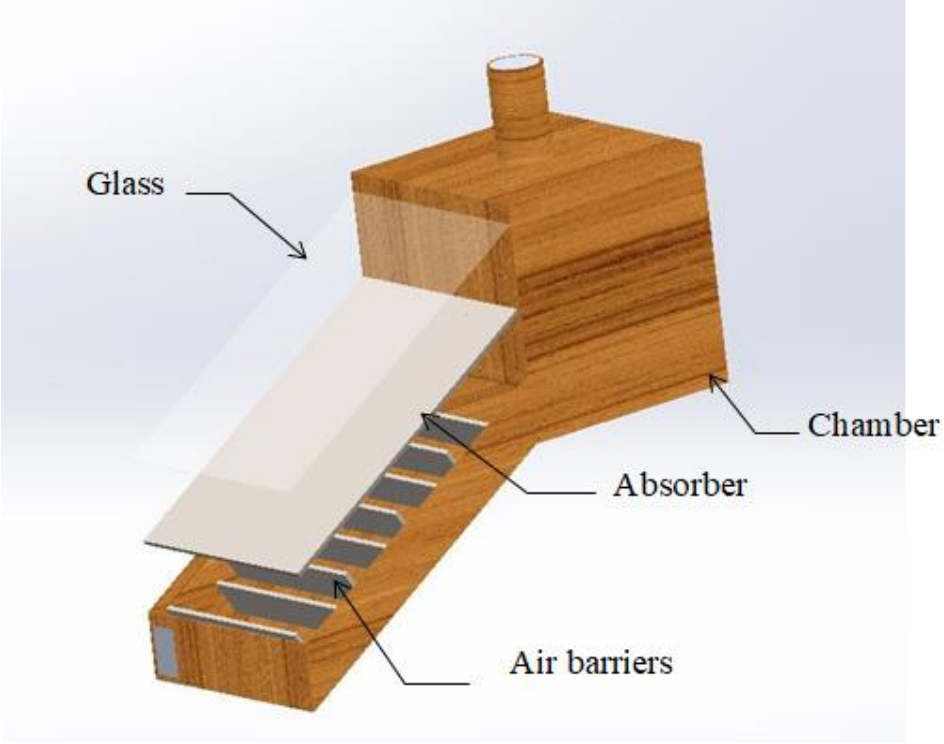

Figure IV.4: indirect solar dryer new model

IV.2.1 Simulation results analysis:

The figure IV.5 represent the simulation results of the new indirect solar dryer in terms of temperature

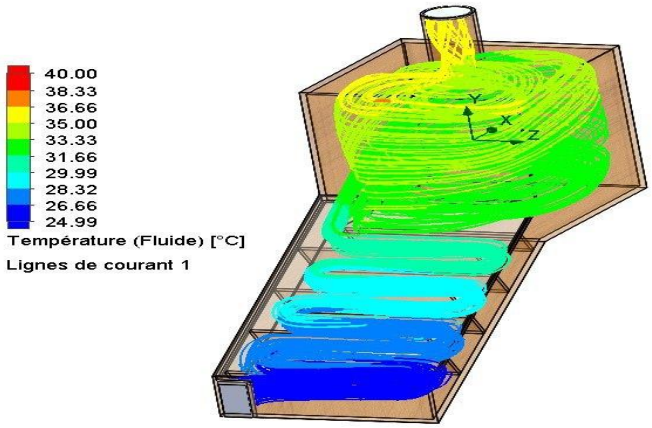

Figure IV.5:Simulation results of the new indirect solar dryer model of temperature

The colors shown in the figure show a gradual distribution of temperatures , with red representing the highest temperature (~40°C) and blue representing the lowest temperature (~24.99°C).

We observe that the air gradually heats up as it passes through the heating channel from left to right, thanks to the presence of an absorbent surface connected to the air baffles to capture thermal energy. The flow follows a long spiral pattern, indicating the use of efficient heat exchangers to gradually raise the air temperature. In the drying chamber, a thermal vortex is formed, improving heat distribution within the chamber, reaching 33°C in the center of the chamber, contributing to homogeneous drying of materials. The spiral path of the air in the chamber increases the air residence time, an important factor in the drying process.

The figure IV.6 shows flow lines (stream lines) colored according to the velocity scale, ranging from 0 to 7.00 m/s. This result represents the airflow generated by natural solar heating inside an indirect solar dryer.

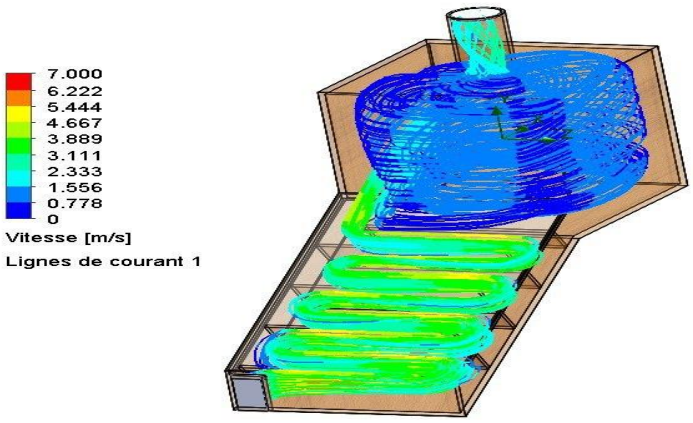

Figure IV.6: Simulation results of the new indirect solar dryer model of air speed

At the beginning of the channel, we observe a relatively low velocity (1.27 m/s), which is consistent with the air being still relatively cold and denser.

As the air advances within the duct and its absorption of heat energy increases, the flow velocity

gradually increases until it reaches the drying chamber at a speed of $3.11 m/s$. As the air enters the vertical chamber, a pronounced spiral (vortex) motion appears.

The irregular velocity distribution is beneficial to the drying process: areas of high velocity ensure continuous air renewal, while lower velocities allow for longer residence times, allowing heat and moisture to be transferred from the dried materials to the surrounding air.

The spiral velocity within the chamber indicates improved mixing of hot air and, consequently, a more homogeneous distribution of heat and moisture, which enhances drying efficiency.

❖ **Comparison of the two designs :**

A table IV.1 representing the results of two studies at limited points :

Table IV.1:Design simulation results

	Prototype of indirect solar dryer	**Improved model of indirect solar dryer:**
fluid temperature (1)	20°C	25°C
fluid Temperature (2)	20°C	31.69°C
fluid Temperature (3)	28.18 °C	33°C
fluid Temperature (4)	27.14 °C	34 °C
fluid Speed (1)	1.73 m/s	1.27 m/s
fluid Speed (2)	1.73 m/s	2.98 m/s
fluid Speed (3)	0.09 m/s	0.44 m/s
fluid Speed (4)	2 m/s	2 m/s

(1) Solar collector entry **(3) Middle of the drying room**

(2) Solar collector exit **(4) When ventilating**

We note that the temperature in the solar collector increased in the improved design. This is due to the air barriers that slowed the air flow and gradually increased its temperature. At the solar collector outlet, it reached 31.69 °C. In the drying chamber, it reached 33 °C,

compared to the initial design, which reached 28.18 °C. This is due to the higher forced convection compared to the initial design and the effect of air movement and speed in the chamber.

Through our study of the two previous designs and the results of their simulation under default conditions, we noticed that the improved design is more efficient than the initial design in several aspects. Therefore, we chose this latter design to conduct a semi-realistic simulation on it.

Through our study in second Chapter on simulating the sun's motion on selected days using the Matlab program, we will simulate the improved design by exploiting the sun's elevation angle and azimuth angle at 10:00AM and noon as shown in table IV.2

Table IV.2: Changes in the azimuth and height angles of the sun

	21st march		**21st June**		**21st December**	
	Azimut:	**H°**	**Azimut:**	**H°**	**Azimut:**	**H°**
10:00AM	59.94°	37.6°	86.98°	52.23°	40.38°	21.74°
At noon	≈ 0°	57.01°	≈ 0°	79.25°	≈ 0°	33.83°

After our internship at the Renewable Energy Center in Ghardaia, we benefited from the data they had that revolved around the temperature and the amount of solar radiation on the days studied.

Measurements were taken on three representative days of the year March 21st , June 21st , and December 21st at two specific times: 10:00 AM and 12:00 PM (noon). On March 21st , the ambient temperature was recorded at 20°C with a Direct Normal Irradiance (DNI) of 800.09 W/m² at 10:00 AM, increasing to 26°C and a DNI of 822.68 W/m² at noon. On June 21st , the temperature rose significantly, with 32°C and a DNI of 670.09 W/m² at 10:00 AM, and reaching 37°C with a DNI of 812.78 W/m² at noon. In contrast, on December 21st , the ambient temperature was much lower, with 10°C and a DNI of 814.41 W/m² at 10:00 AM, rising slightly to 15°C and a DNI of 933.49 W/m² at noon. These variations reflect the seasonal and diurnal changes in solar irradiance and ambient conditions throughout the year.[37]

IV.2.2 Semi-realistic simulation :

IV.2.2.1 Simulation results for March 21st:

Figure IV.7 represents the changes in air velocity (left) and liquid temperature (right) on March 21st at 10:00 a.m.

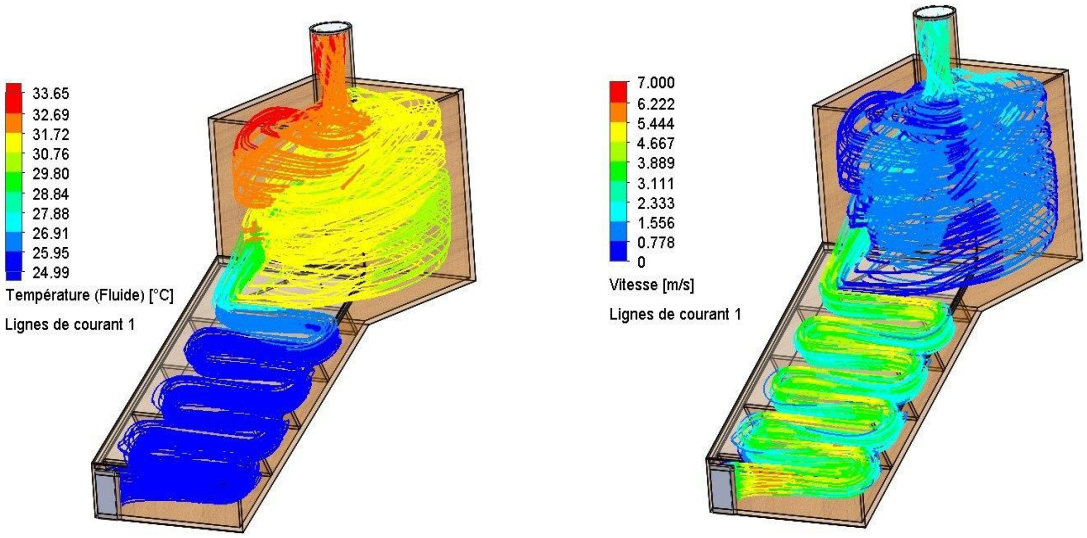

Figure IV.7:Air speed and temperature changes on march 21st at 10:00AM

During the morning at 10:00, the indirect solar dryer demonstrated relatively limited performance. Air temperatures gradually increased in the solar collector due to the absorber and air barriers, reaching a temperature of 31°C. This was due to the low air velocity of 0.60 m/s and stagnation in the chamber. This relatively poor performance is attributed to the low solar radiation intensity during this time of day, as the angle of incidence of sunlight on the solar collector is still oblique, reducing the amount of thermal energy absorbed by the absorber. This lack of available energy resulted in insufficient air heating and, consequently, a slowdown in the drying process inside the chamber. It can be concluded that the prevailing climatic conditions in the morning do not provide optimal conditions for an efficient drying process.

Figure IV.8 represents the changes in air velocity (left) and liquid temperature (right) on March 21st at noon

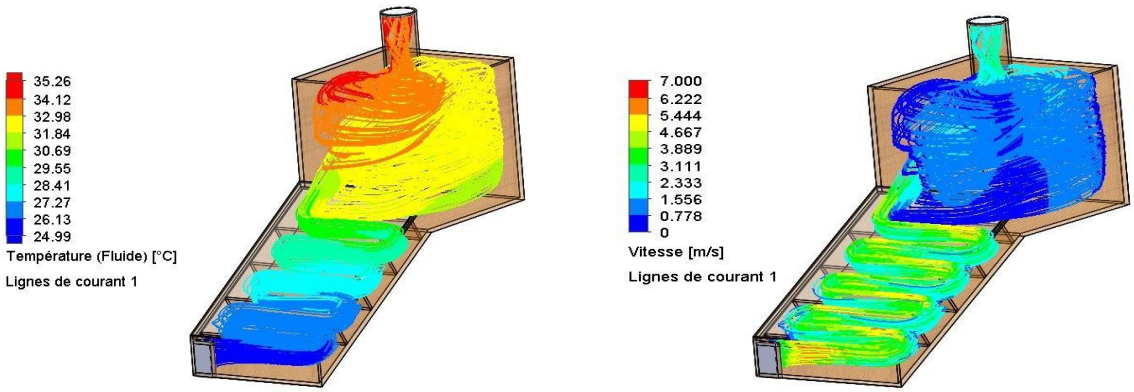

Figure IV.8: Air speed and temperature changes on march 21st at noon

Experimental measurements showed that the indirect solar dryer performed with high thermal efficiency and a high drying rate during the afternoon (12:53). The air temperature entering the drying chamber rose by 32°C, reaching 33.44°C at the center of the chamber, with the air velocity decreasing to 0.37 m/s. This optimal performance is attributed to the position of the sun, which increased the solar radiation intensity to 822.68 W/m². This enabled the solar collector to absorb a greater amount of thermal energy and convert it into heat, increasing the temperature difference between the inside and outside of the dryer, a key factor in activating and regulating natural convection currents. The results indicate that the afternoon is the most suitable time for solar drying using the indirect dryer, especially on sunny days, to achieve higher energy efficiency and accelerate the drying process.

IV.2.2.2 Simulation results for june 21st :

Figure IV.9 represents the changes in air velocity (left) and liquid temperature (right) on june 21st at 10:00 a.m.

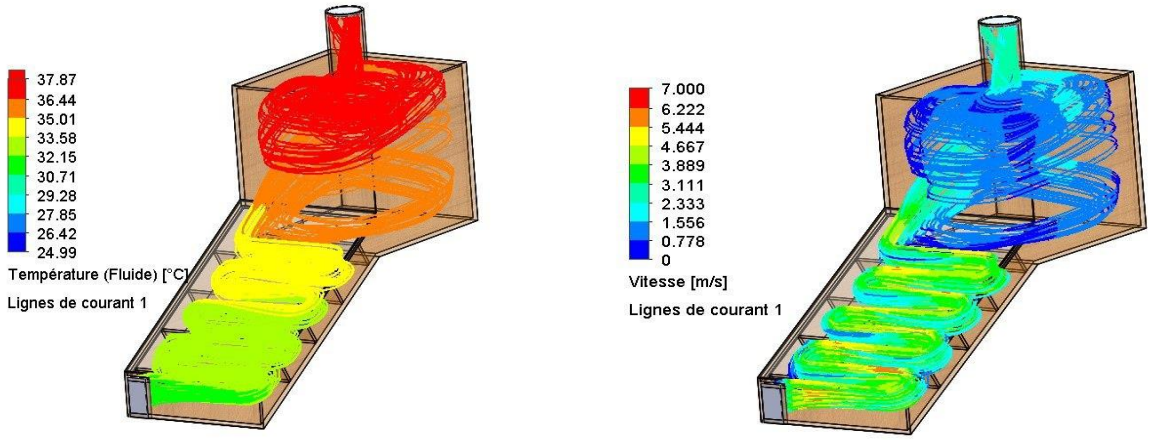

Figure IV.9:Air speed and temperature changes on june 21st at 10:00AM

At 10:00 a.m., the air temperature in the solar collector gradually rose to 36.02°C, as energy was absorbed by the collector and air baffles. The air velocity decreased to 0.44 m/s, and the air inside the chamber remained stagnant. This performance was attributed to the solar radiation intensity of 670.09 W/m² and the oblique angle of incidence on the collector, which reduced the amount of thermal energy absorbed. Nevertheless, this result was satisfactory under these conditions.

Figure IV.10 represents the changes in air velocity (left) and liquid temperature (right) on june 21st at noon.

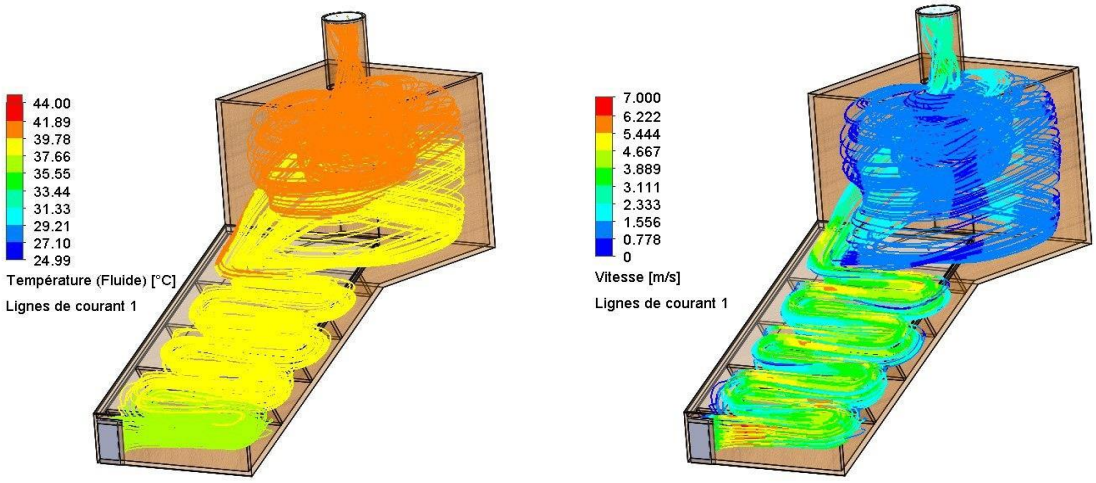

Figure IV.10: Air speed and temperature changes on june 21st at noon

We observed that the indirect solar dryer achieved high thermal efficiency and a high drying rate during the afternoon (12:40). The air temperature entering the drying chamber increased by 38.30°C, reaching 39.50°C at the center of the chamber, with the air velocity decreasing to 0.46 m/s. This optimal performance is attributed to the position of the sun, which increased the solar radiation intensity to 812.78 W/m². This enabled the solar collector to absorb a greater amount of thermal energy and convert it into heat, increasing the temperature difference between the inside and outside of the dryer, a key factor in activating and regulating natural convection currents. The results indicate that the afternoon is the most suitable time for solar drying using the indirect dryer, especially on sunny days, to achieve higher energy efficiency and accelerate the drying process.

IV.2.2.3 Simulation results for December 21st :

Figure IV.11 represents the changes in air velocity (left) and liquid temperature (right) on December 21st at 10:00 a.m.

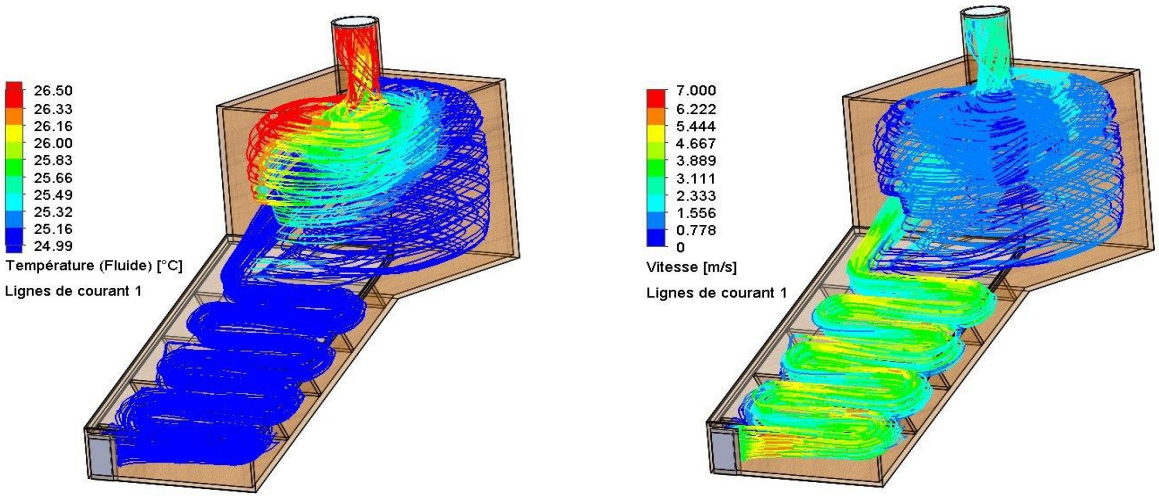

Figure IV.11:Air speed and temperature changes on December 21st at 10:00AM

We observed that the indirect solar dryer performed relatively poorly in the morning at 10:00 AM. At the collector inlet, the ambient temperature was 10°C, and the air temperature in the collector gradually rose to 21°C due to thermal absorption and air barriers , reaching 25.10°C at the center of the chamber. The air velocity dropped to 0.48 m/s, and the room experienced stagnation. This poor performance was attributed to the low solar radiation intensity at this time due to the oblique angle of the sun's rays, which reduced the amount of thermal energy absorbed despite the high solar irradiance of 814 W/m². This energy deficiency resulted in insufficient air heating and a slower drying process. Therefore, morning climatic conditions are not ideal for efficient drying.

Figure IV.12 represents the changes in air velocity (left) and liquid temperature (right) on December 21st at noon.

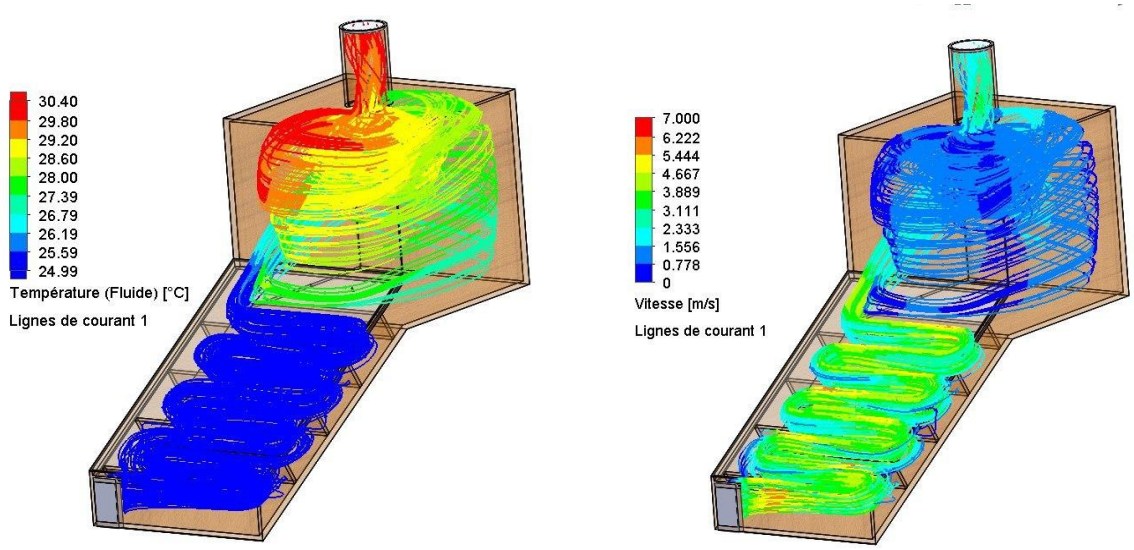

Figure IV.12: Air speed and temperature changes on December 21st at noon

The indirect solar dryer demonstrated high thermal efficiency and a high drying rate at noon (12:42). The air temperature entering the drying chamber increased by 25.72°C and reached 27.83°C at the center of the chamber, with the air velocity decreasing to 0.43 m/s. This optimal performance is attributed to the position of the sun, which increased the solar radiation intensity to 933.49 W/m² and the ambient temperature by 15°C compared to the morning. This enabled the solar collector to absorb a greater amount of thermal energy and convert it into heat, increasing the temperature difference between the inside and outside of the dryer, a key factor in activating natural convection currents. The results indicate that noon is the most suitable time for solar drying using the indirect dryer on sunny days, achieving higher energy efficiency and accelerating the drying process.

- **Compare simulated results :**

Figure IV.13 Represents a bar graph of the changes in dryer temperature during the study days in two hours.

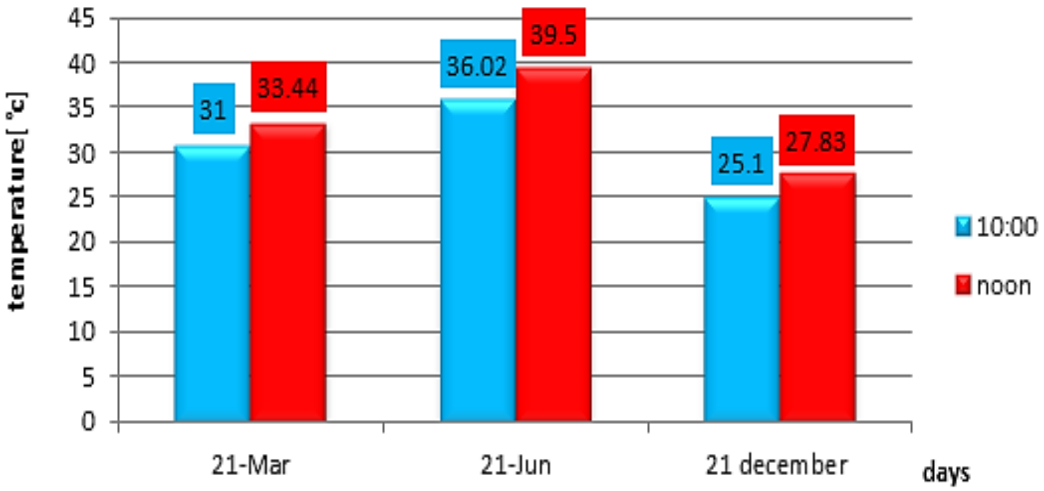

Figure IV.13:Temperature changes inside the dryer chamber on the studied days

This represents a bar graph of the two-hour changes in dryer temperature during the study days. The experimental results on the performance of the indirect solar dryer with a single collector showed that drying efficiency was better during the afternoon compared to the morning (10:00). A significant increase in the temperature of the air entering the dryer was recorded during the afternoon, which positively impacted drying efficiency.

This improvement in performance is primarily due to the prevailing climatic factors during that period. The intensity of solar radiation peaked at noon, leading to greater absorption of thermal energy by the solar collector, thus increasing the temperature of the air entering the dryer. This increased temperature enhanced the drying process and helped accelerate heat transfer from the air to the product. From the bar chart, we can see that drying efficiency in

June is higher than in March and December. This is due to the sun's elevation angle, azimuth angle, and ambient temperature. Therefore, it can be said that climatic conditions during the midday period are more favorable for effective drying. This demonstrates the importance of choosing the right drying timing to improve system efficiency, especially when using a solar-powered dryer that directly depends on environmental variables.

In the initial design, we used a single solar collector to capture and convert solar energy, which achieved good results in most cases. However, we wanted to achieve higher thermal efficiency and increase drying rates. We were drawn to the idea of adding a second solar collector, so that the two collectors would work together to enhance solar energy absorption and increase the amount of heat transferred to the drying chamber.

The basic idea behind using two solar collectors is to improve system performance by increasing the surface area absorbing solar radiation, thereby increasing the amount of thermal energy produced. This is what we will address in our new study.

IV.3 model of indirect solar dryer with two collectors :

The basic idea behind using two identical solar collectors is to improve system performance by increasing the surface area absorbing solar radiation

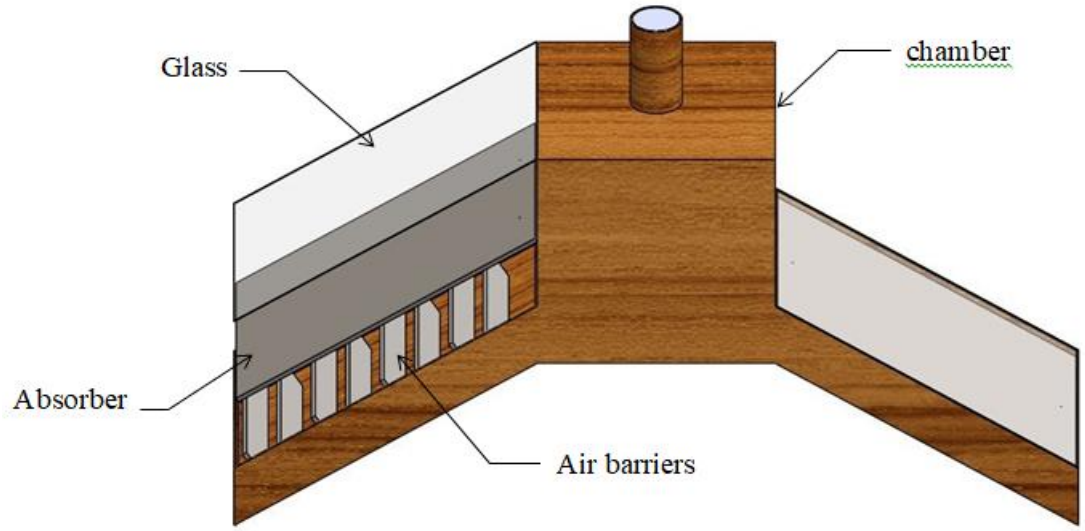

Figure IV.14:indirect solar dryer with two solar collectors

The design of an indirect solar dryer with two solar collectors, along with its thermal performance analysis, will be presented during the selected study days.

IV.3.1 Simulation results for March 21st :

Figure IV.15 represents the changes in air velocity (left) and liquid temperature (right) on march 21st at 10:00 a.m for two collectors.

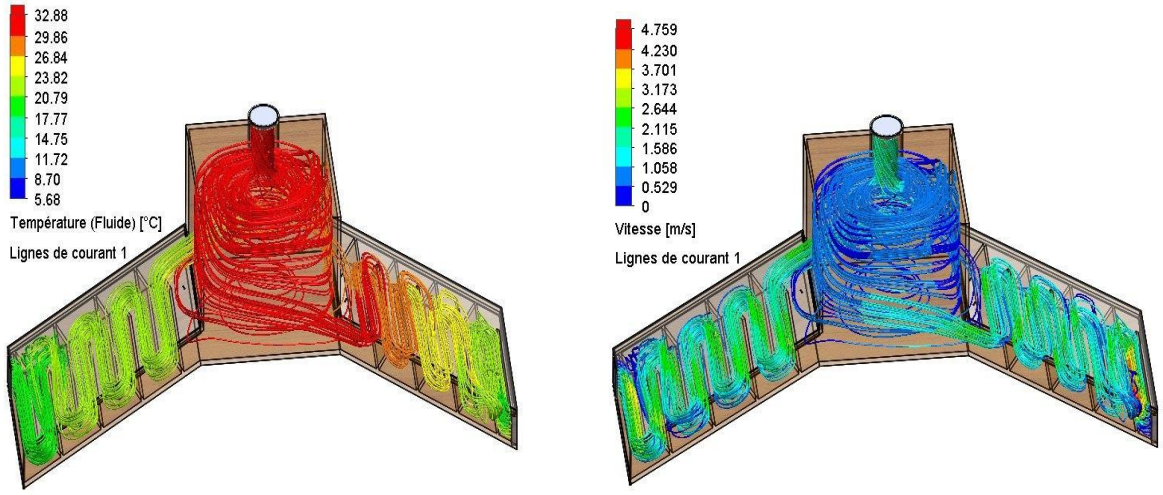

Figure IV.15:Air speed and temperature changes on march 21st at 10:00AM (2collectors)

Figure IV.16 represents the changes in air velocity (left) and liquid temperature (right) on march 21st at noon for two collectors.

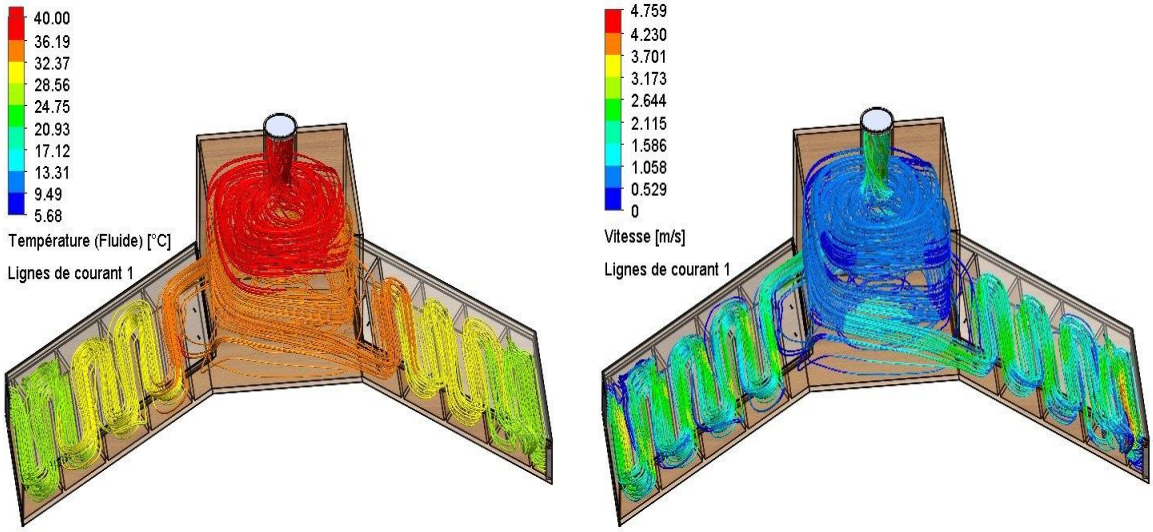

Figure IV.16:Air speed and temperature changes on march21st at noon(2collectors)

- **Analysis and interpretation of results (march 21st) :**

The performance results of an indirect solar dryer equipped with two solar collectors during two main periods of the day: 10:00 a.m. and 12:35 p.m. The results showed that its performance in the morning was less efficient than in the afternoon, in terms of the air temperature entering the drying chamber. middle of the chamber reached 30.25°C. This decline in performance during the morning is related to several factors. At this time, the angle of incidence of solar radiation is relatively low, affecting the collectors' ability to efficiently absorb solar energy, even with the larger surface area provided by two collectors.

Consequently, the incoming air temperature remains below the level required for effective drying.

the dryer demonstrated significantly improved performance during the midday period, taking advantage of the nearly vertical position of the sun, which enabled the collectors to absorb more radiation and convert it into heat. This resulted in a significant increase in the inlet air temperature of 35.63°C, which helped enhance convection currents within the system.

IV.3.2 Simulation results for June 21st:

Figure IV.17 represents the changes in air velocity (left) and liquid temperature (right) on June 21st at 10:00 a.m for two collectors.

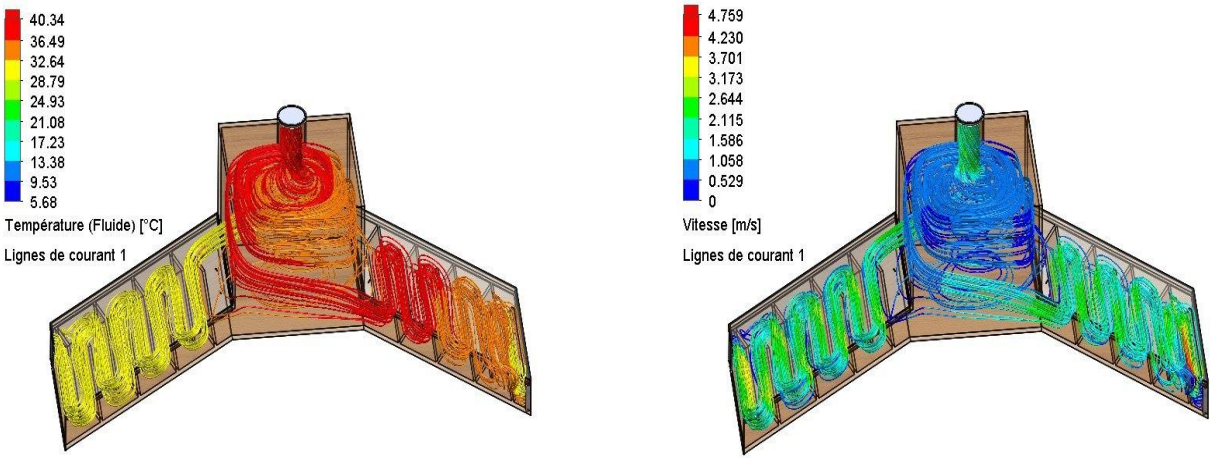

Figure IV.17:Air speed and temperature changes on june 21st at 10:00AM (2collectors)

Figure IV.18 represents the changes in air velocity (left) and liquid temperature (right) on June 21st at noon for two collectors.

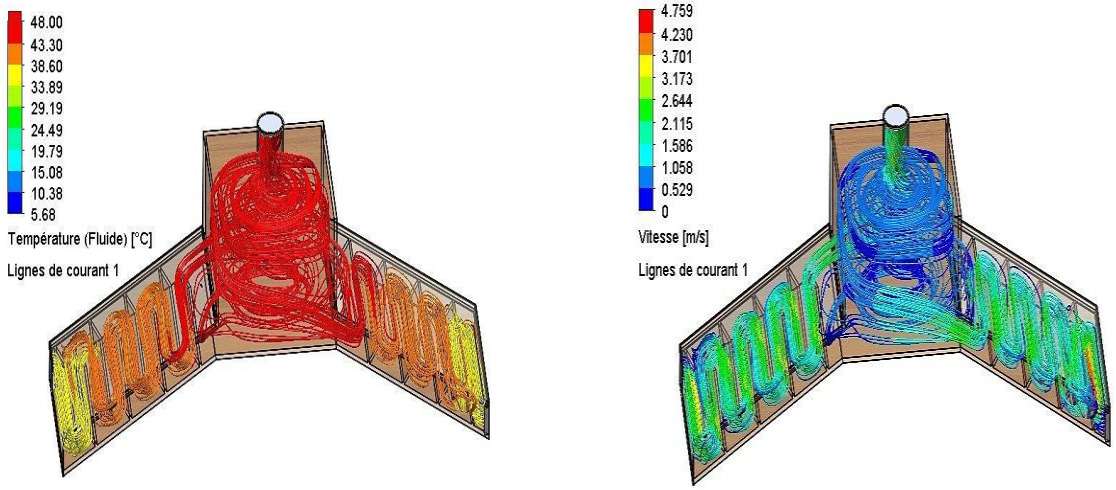

Figure IV.18:Air speed and temperature changes on june 21st at noon (2collectors)

- **Analysis and interpretation of results (June 21st) :**

When we studied the performance of an indirect solar dryer equipped with two solar collectors on June 21st during two main periods of the day: morning at 10:00 a.m. and midday at 12:40 p.m, the results showed that its performance was less efficient in the morning than in the midday period, in terms of the air temperature entering the drying chamber. The temperature in the center of the chamber reached 35.45°C. This decrease in performance during the morning is related to several factors. At this time, the angle of incidence of solar radiation is relatively low, affecting the ability of the collectors to absorb solar energy. The collector facing the sun absorbs more, reaching 37.08°C at the collector exit compared to 32.43°C at the other collector. This temperature difference led to a gradual decrease in the center of the chamber, reaching 35.45°C, even with the larger surface area provided by the two collectors.

In contrast, the dryer showed a significant improvement in performance during the afternoon, taking advantage of the sun's near-vertical position, which enabled the collectors to absorb more radiation and convert it to heat almost uniformly. This resulted in a significant increase in the inlet air temperature to 44.56°C, which helped enhance convection currents within the system.

IV.3.3 Simulation results for December 21st :

Figure IV.19 represents the changes in air velocity (left) and liquid temperature (right) on December 21st at 10:00 a.m for two collectors.

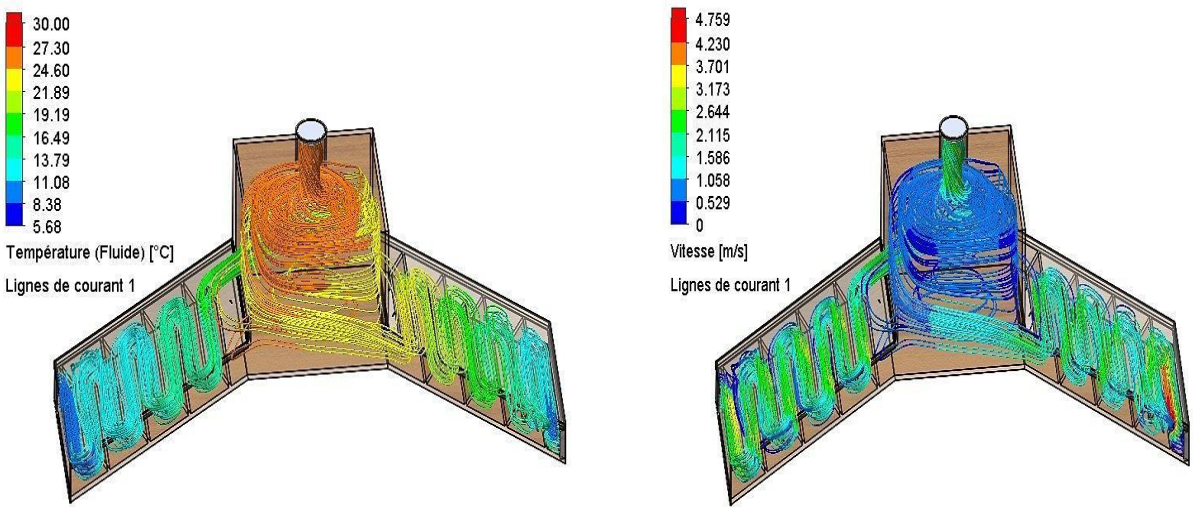

Figure IV.19:Air speed and temperature changes on December 21st at 10:00AM (2collectors)

Figure IV.20 represents the changes in air velocity (left) and liquid temperature (right) on December 21st at noon for two collectors.

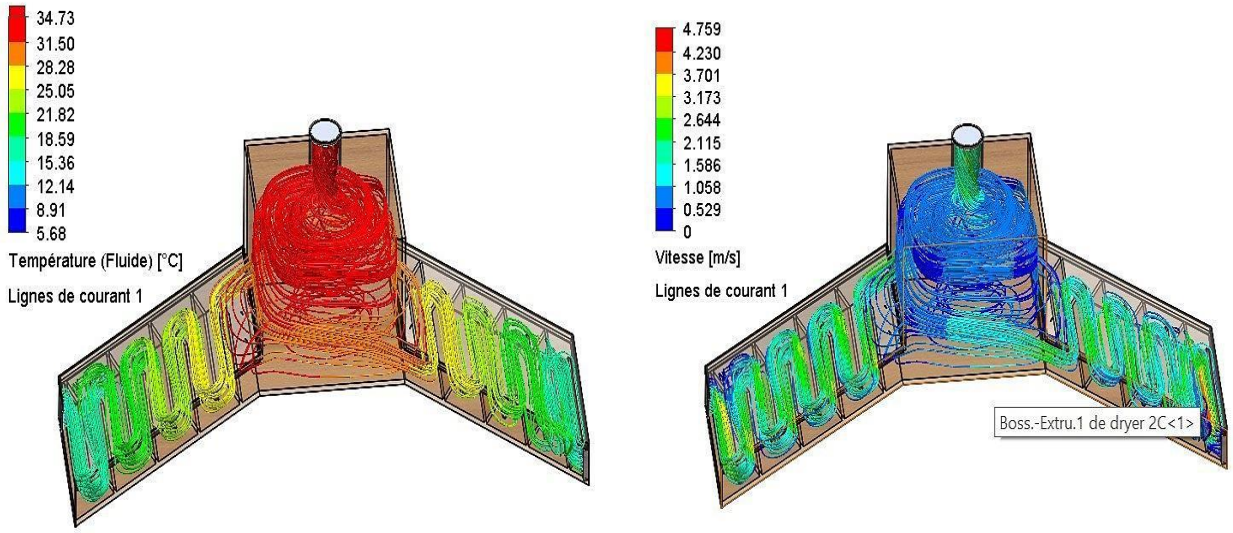

Figure IV.20:Air speed and temperature changes on December 21st at noon (2collectors)

- **Analysis and interpretation of results (December 21st) :**

A study on December 21st examined the performance of an indirect solar dryer equipped with two solar collectors during two key periods: morning at 10:00 a.m. and afternoon at 12:42 PM. The results showed that the dryer performed less efficiently in the morning than in the afternoon, in terms of the air temperature entering the drying chamber. The temperature at the center of the chamber reached 24.52°C. This decrease in performance during the morning is related to several factors. At this time, the angle of incidence of solar radiation is relatively low, affecting the collectors' ability to absorb solar energy. The collector facing the sun absorbed more energy, reaching 23.27°C at the collector exit, compared to 19.81°C at the other collector. The temperature reached 24.52°C at the center of the chamber. In contrast, the dryer showed a significant improvement in performance during the afternoon, benefiting from the sun's near-vertical position, which enabled the collectors to absorb more radiation and convert it to heat more uniformly. This resulted in a significant increase in the incoming air temperature to 31.93°C, which contributed to enhanced convection currents within the system.

- **Compare simulated results**

Figure IV.21 Represents a bar graph of the changes in dryer temperature during the study

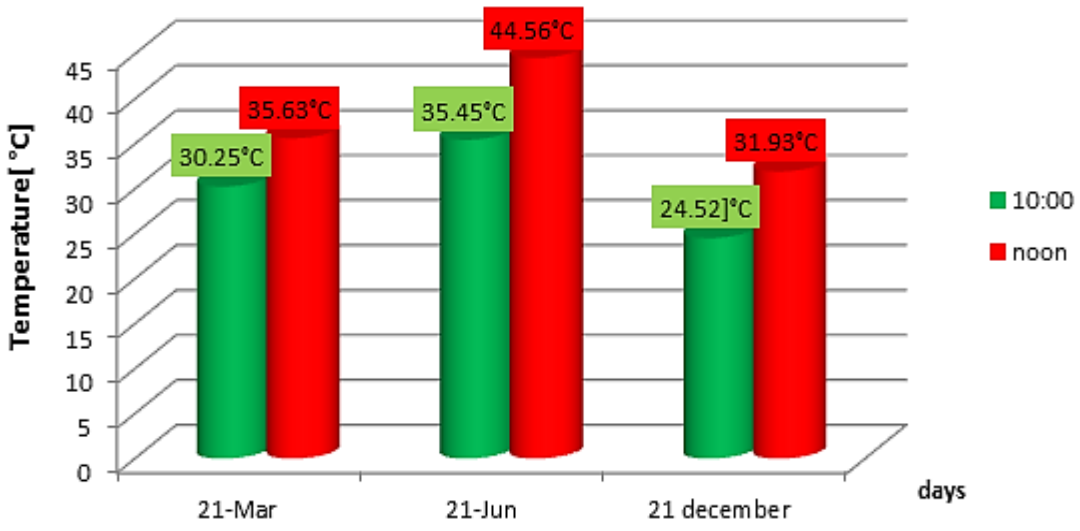

Figure IV.21: Temperature changes inside the dryer on the studied days (2collectors)

This represents a bar graph of the two-hour changes in dryer temperature over the study days. The experimental results of the indirect solar dryer with two collectors showed that drying efficiency was better during the midday period compared to the morning (10:00 AM). A significant increase in the air temperature entering the dryer was recorded during the midday period, which positively impacted drying efficiency.

This improved performance is primarily due to the prevailing climatic factors during that period. The solar radiation intensity peaked at noon, resulting in greater absorption of thermal energy by the solar collector, thus increasing the air temperature entering the dryer. This increased temperature enhanced the drying process and helped accelerate heat transfer from the air to the product. From the bar graph, we can see that the drying efficiency in June was higher than in March and December at 10:00 AM and midday, reaching 35.45°C and 44.56°C, respectively. This is due to the sun's elevation angle, azimuth angle, and ambient temperature. Therefore, it can be said that climatic conditions during the afternoon are more favorable for efficient drying. This highlights the importance of choosing the appropriate drying timing to optimize system efficiency, especially when using a solar-powered dryer that directly depends on environmental variables.

Based on these results, it can be concluded that increasing the number of collectors alone is not sufficient to ensure high efficiency at 10:00 AM for a single collector. The radiation intensity and angle of incidence, along with the ambient temperature, remain critical factors, especially in an indirect drying system. Therefore, the timing of solar dryer operation remains one of the key determinants of its effectiveness, even when using an improved system with two thermal collectors.

Using two solar collectors to capture and convert solar energy yielded relatively good results in most cases. However, we wanted to achieve higher thermal efficiency and increase drying rates. We were attracted to the idea of adding a third solar collector, so that the collectors would work together to enhance solar energy absorption and increase the amount of heat transferred to the drying chamber.

The idea behind using three solar collectors is to improve system performance by increasing the surface area absorbing solar radiation, thereby increasing the amount of thermal energy produced. This is what we will address in our new study.

IV.4 Model of indirect solar dryer with three collectors:

The second idea behind using three identical solar collectors is to improve the system's performance by increasing the surface area that absorbs solar radiation compared to previous designs.

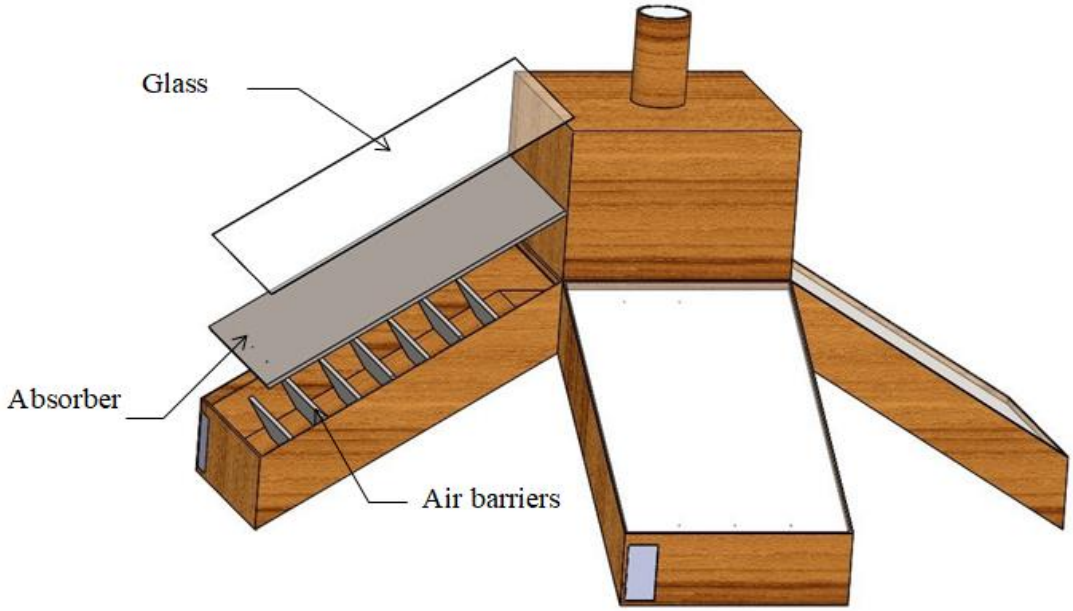

Figure IV.22:indirect solar dryer with three solar collectors

IV.4.1 Simulation results for March 21st:

Figure IV.23 represents the changes in air velocity (left) and liquid temperature (right) on March 21st at 10:00 a.m for three collectors.

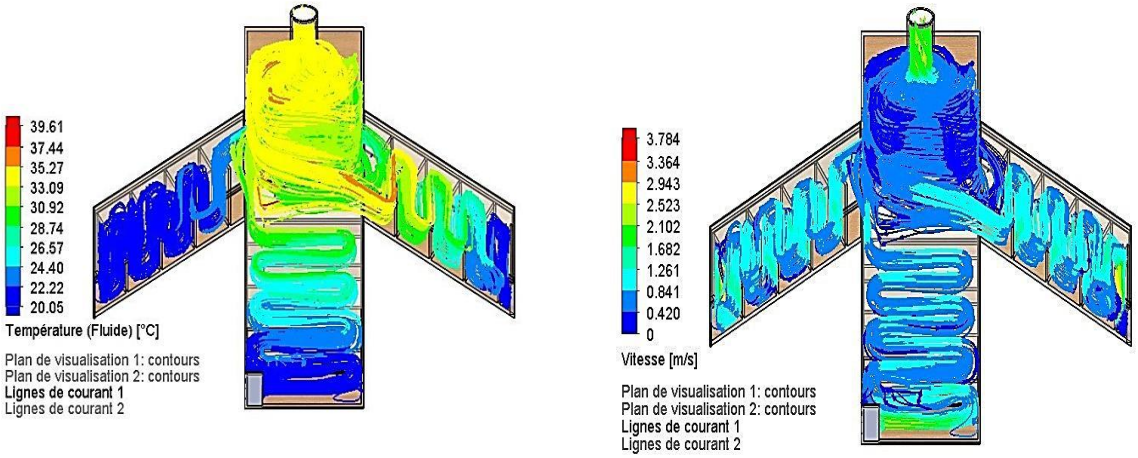

Figure IV.23:Air speed and temperature changes on march 21st at 10:00AM (3collectors)

Figure IV.24 represents the changes in air velocity (left) and liquid temperature (right) on march 21st at noon for three collectors.

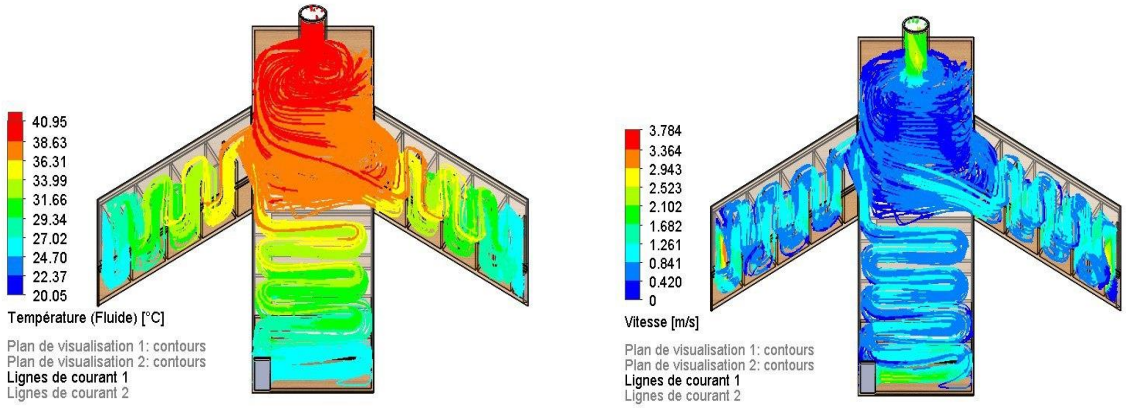

Figure IV.24:Air speed and temperature changes on march 21st at noon(3collectors)

- **Analysis and interpretation of results (march 21st) :**

The results show that the efficiency of a solar dryer varies significantly between 10 a.m. and noon, due to changes in climatic and radiation characteristics throughout the day. At 10 a.m the sun's inclination angle is greater (the sun is closer to the horizon), meaning the amount of solar radiation falling on the collectors is relatively lower. A larger portion of the solar radiation is reflected off the collector surface and not fully absorbed, resulting in a decrease in the amount of heat produced. We note that there is a difference in the absorption of radiation by the absorbers, leading to slower heating of the air within the system. In the first absorber, the air temperature upon exiting the first collector reached 32°C, while in the second, it reached 35.67°C. This is due to both taking advantage of the sun's position. In the third collector, it reached 24.72°C because it does not receive as much sunlight. This affects the room temperature due to the difference in the amount of sunlight received to heat the air. This resulted in the room temperature reaching 31.40°C. This is compared to noon, when the

sun is at its highest point (nearly vertical approach angle). This enables the collectors to receive more direct and stronger solar radiation. Also, the ambient temperature at noon is higher due to the heat buildup during the morning hours, which reduces the temperature difference between the heated air in the collector and the ambient temperature, thus reducing heat loss and improving the dryer's performance, as the air temperature inside the room reached 37.53°C**.**

IV.4.2 Simulation results for June 21st:

Figure IV.25 represents the changes in air velocity (left) and liquid temperature (right) on June 21st at 10:00 a.m for three collectors.

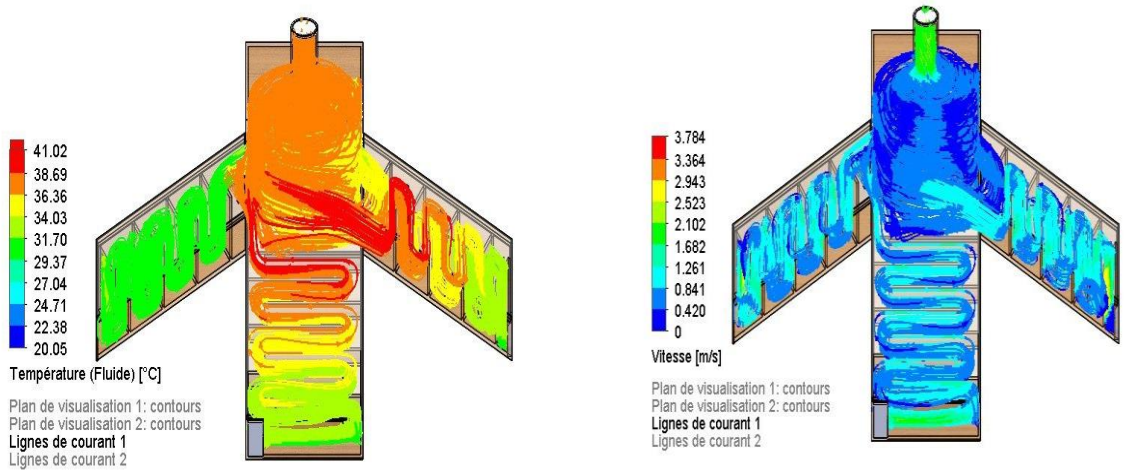

Figure IV.25:Air speed and temperature changes on june 21st at 10:00AM (3collectors)

Figure IV.26 represents the changes in air velocity (left) and liquid temperature (right) on June 21st at noon for three collectors.

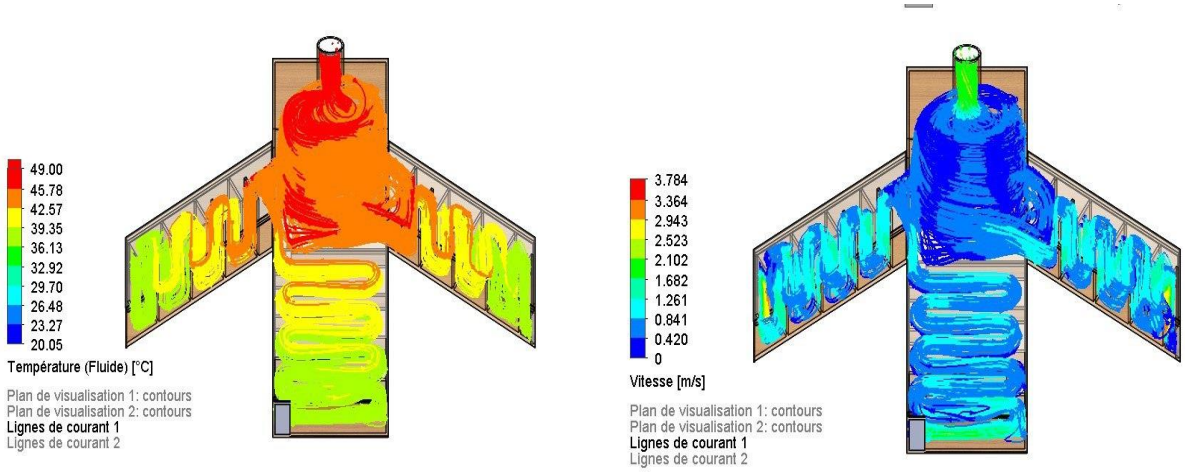

Figure IV.26: Air speed and temperature changes on june 21st at noon (3collectors)

- **Analysis and interpretation of results (June 21st) :**

We observe that the efficiency of the solar dryer varies significantly between 10 a.m. and noon, due to changes in climatic and radiation characteristics throughout the day. At 10 a.m., the sun's angle of inclination is greater (the sun is closer to the horizon), meaning that the amount of solar radiation falling on the collectors is relatively lower. A greater portion of the solar radiation is reflected from the collector surface and not fully absorbed, resulting in a lower amount of heat produced. We observe a difference in the absorption of radiation by the absorbers, resulting in slower heating of the air within the system. In the first absorber, the air temperature upon exiting the first collector reached 37.06°C, while in the second, it reached 38.06°C. This is due to both benefiting from the position of the sun. In the third collector, it reached 32.83°C, almost the same as the ambient temperature because it does not receive as much sunlight. This affects the room temperature due to the difference in the amount of sunlight received to heat the air. This resulted in the room temperature reaching 36.28°C .At noon, when the sun is at its highest point. This allows the collectors to receive more direct and intense solar radiation. The ambient temperature at noon is also higher due to the heat buildup during the morning hours, at 37°C. This reduces the temperature difference between the heated air in the collector and the ambient temperature, reducing heat loss and improving dryer performance. The air temperature inside the room reached 45.03°C. This is due to the air stagnation of 0.23 m/s

IV.4.3 Simulation results for December 21st:

Figure IV.27 represents the changes in air velocity (left) and liquid temperature (right) on December 21st at 10:00 a.m for three collectors.

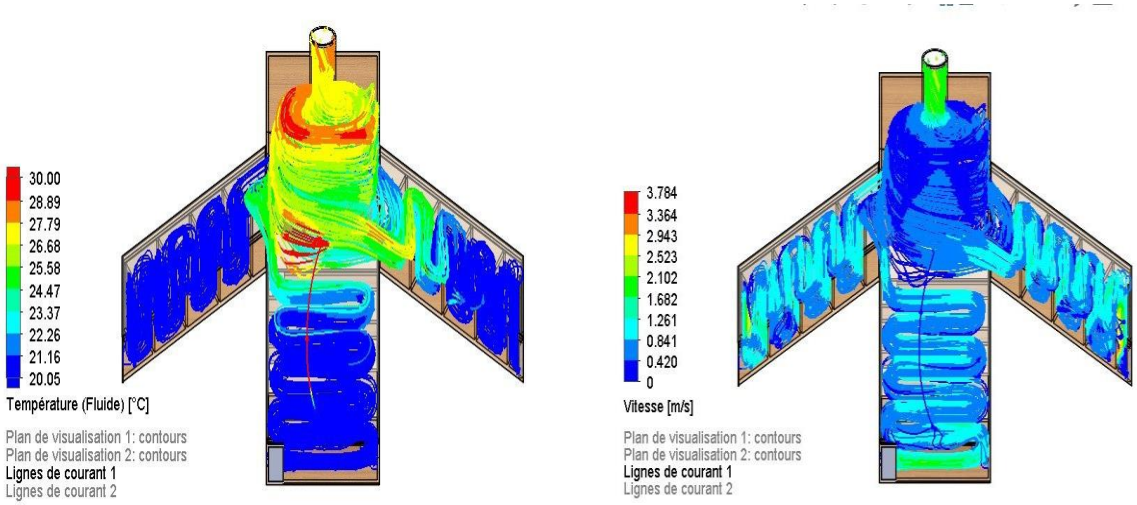

Figure IV.27: Air speed and temperature changes on December 21st at 10:00AM (3collectors)

Figure IV.28 represents the changes in air velocity (left) and liquid temperature (right) on December 21st at noon for three collectors.

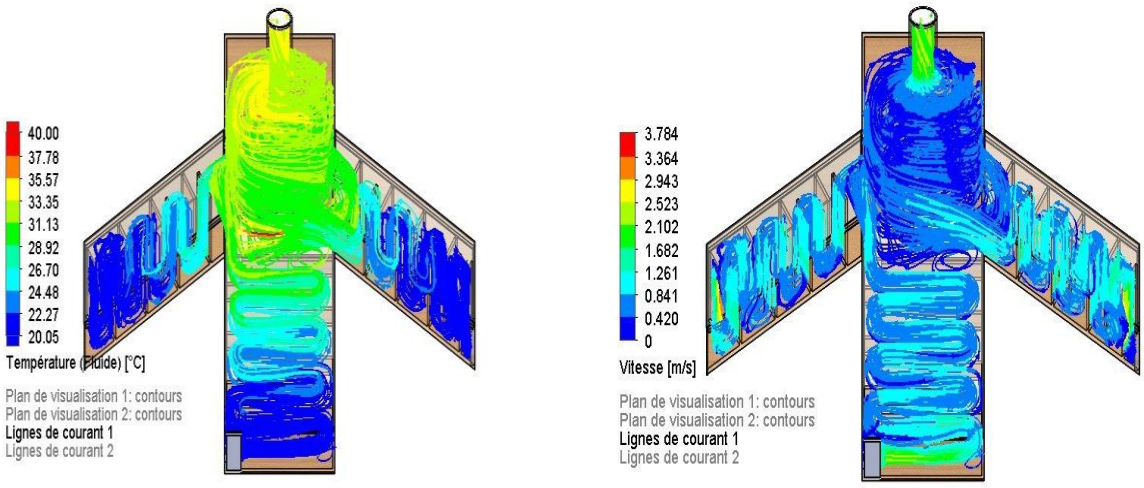

Figure IV.28: Air speed and temperature changes on December 21st at noon (3collectors)

- **Analysis and interpretation of results (December 21st) :**

Dryer performance varies between 10 a.m. and noon, due to changes in climatic and radiation characteristics throughout the day. At 10 a.m., the sun's angle is greater. meaning the amount of solar radiation falling on the collectors is relatively lower. A greater portion of the solar radiation is reflected from the collector surface and not fully absorbed, resulting in less heat production. We observe a difference in the absorption of radiation by the absorbers, and the cooler ambient temperature leads to slower heating of the air within the system. This affects the room temperature due to the difference in the amount of sunlight received to heat the air. This resulted in a room temperature of 25.20°C despite the high solar radiation of 814.41°C .At noon, when the sun is at its highest point. This allows the collectors to receive 933.49°C more direct and intense solar radiation. The ambient temperature at noon is also slightly higher due to the heat accumulation during the morning hours, which is 15°C higher. This reduces the temperature difference between the heated air in the collector and the ambient temperature, reducing heat loss and improving dryer performance. The air temperature inside the room reached 32.1°C. This is due to air stagnation of 0.25 m/s.

- **Compare simulated results**

Figure IV.29 represents a bar graph of the changes in dryer temperature during the days

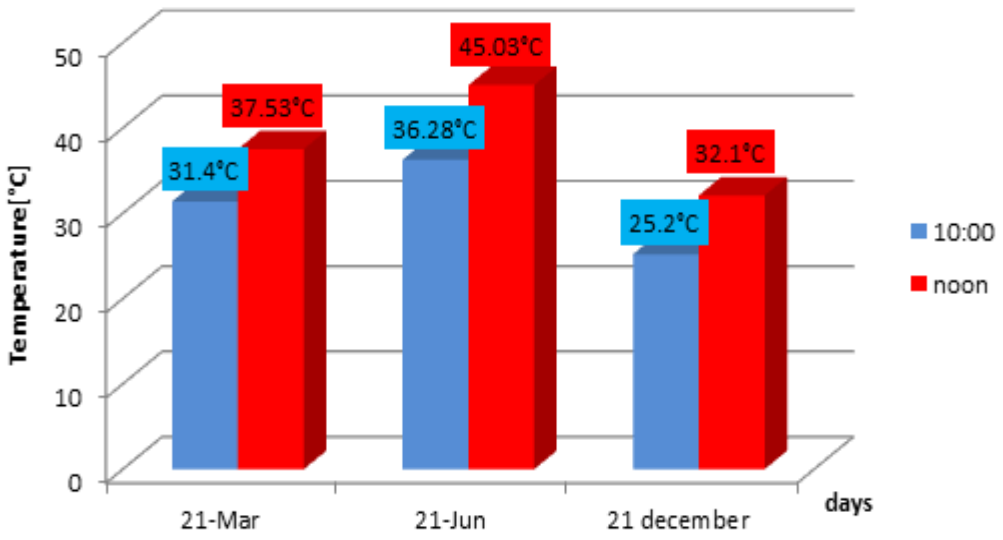

Figure IV.29: Temperature changes inside the dryer chamber on the studied days (3collectors)

The bar graphs in the figure represent the results of temperature measurements inside an indirect solar dryer equipped with three thermal collectors during three pivotal days of the year:21st March (vernal equinox), 21st June (summer solstice), and 21st December (winter solstice), and at two specific time periods: 10:00 a.m. and noon. The results showed that the highest temperature recorded was on 21st June, reaching 36.28°C in the morning and 45.03°C at noon, indicating high efficiency in absorbing solar radiation during the summer due to the nearly perpendicular angle of incidence and the increased intensity of solar radiation. In contrast, temperatures recorded on 21st March were relatively lower, reaching 31.4°C in the morning and 37.53°C at noon. The lowest values were recorded on 21st December, reaching 25.2°C in the morning and 32.1°C at noon, consistent with the significant decrease in ambient temperature during the winter. These results reflect the direct impact of changing sun angles and varying solar radiation levels on solar dryer performance. Maximum efficiency is achieved during the summer months, when ambient temperatures are higher, resulting in faster heat generation inside the dryer compared to spring and winter. Ambient temperature plays a significant role in supporting the heating efficiency inside a solar dryer, as the temperature difference between the indoor and outdoor air increases.

IV.5 Discussion of results:

Based on our previous design studies, we aim to compare the performance of three solar dryer models: a single-collector dryer, a double-collector dryer, and a triple-collector dryer. This comparison is based on several criteria, including the rate of temperature rise within the drying chamber, thermal stability, and overall system efficiency. Through this study, we can

assess the impact of increasing the number of solar collectors on improving dryer performance.

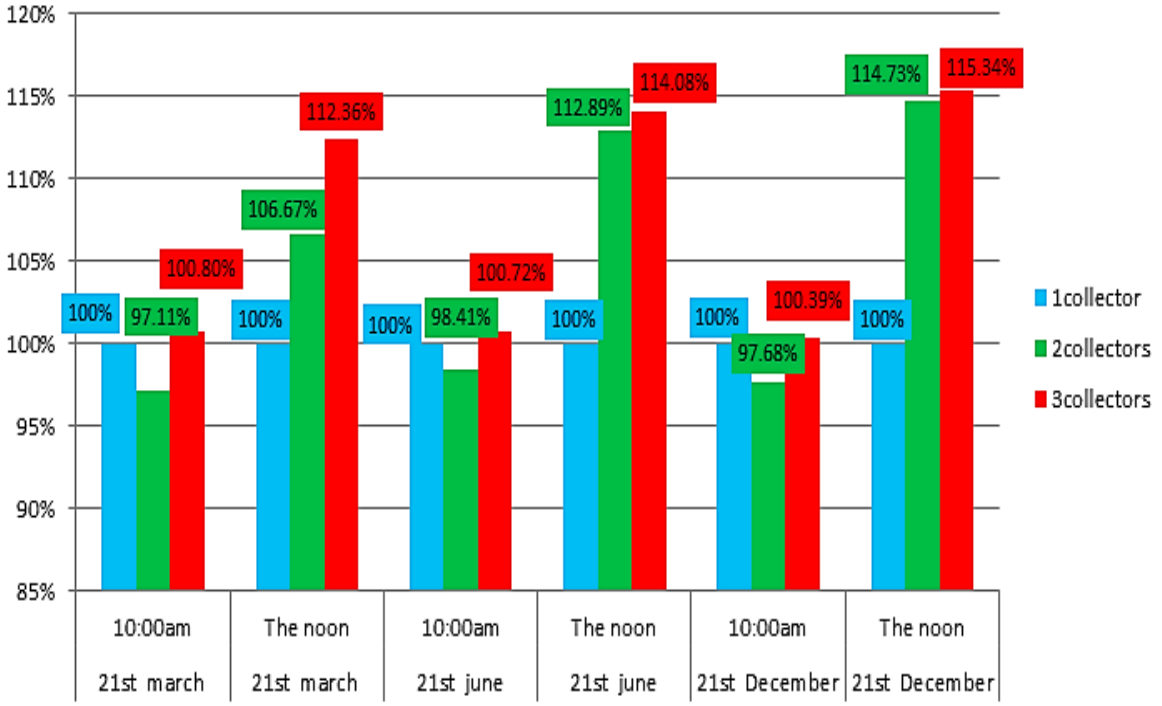

Figure IV.30:Compare designs in terms of room temperature

The bar graph in Figure IV.30 illustrates the relative performance improvement of two alternative indirect solar dryer designs: one with two collectors and one with three collectors compared to the baseline system equipped with a single collector (100% uniformity). The simulations were conducted on three representative solar dates (March 21st , June 21st , and December 21st) at two specific times: 10:00 a.m. and noon.

At all times and dates, the two- and three-collector systems performed better than the single-collector system. On March 21st , the two-collector system achieved 97.11% performance at 10:00 a.m. and 106.67% at noon, while the three-collector system achieved 100.80% and 112.36%, respectively. The improvement at noon reflects the benefits of increased solar radiation and ambient temperature.

On June 21st , despite being the hottest day, performance at 10:00 a.m. remained relatively modest (98.41% for the two collectors and 100.72% for the three collectors), due to the low DNI at that time. However, performance improved significantly at noon, reaching 112.89% and 114.08%, respectively.

It is worth noting that on December 21st , despite the low ambient temperatures, the system demonstrated superior performance thanks to the high DNI. At 10:00 a.m., the values reached 97.68% and 100.39% for the two and three collectors, respectively. At noon, performance

peaked: 114.73% for the two-collector design and 115.34% for the three-collector design. By comparing performance across the three days,

We found that the efficiency of a solar dryer is primarily affected by three interconnected factors:

- Number of collectors: This has a direct impact on increased heat production, especially during peak solar periods.
- Time of day: Performance is best at noon in all cases, due to the larger angle of incidence.
- Season and ambient temperature: These play a crucial role in the effectiveness of heat transfer. We observed that performance was at its peak during the summer (June), when ambient temperatures are high, and decreased in the winter (December), when the cold weather delays the drying process.

CONCLUSION:

Using a larger number of collectors enhances the efficiency of a solar dryer, but efficiency Maximum efficiency is achieved only when conditions of optimal solar radiation and high ambient temperatures are present. Therefore, planning the dryer's usage schedule throughout the day and year is a crucial factor in achieving maximum energy and thermal efficiency.

General Conclusion

CONCLUSION:

In this study, we concluded that the indirect solar dryer equipped with solar collectors is an effective and sustainable alternative for drying agricultural products, especially in areas with high solar radiation. Experimental results showed that system performance significantly improves with increasing the number of solar collectors, particularly during the afternoon and summer months, when the indoor temperature ranged from 39.47 to 45.03°C, where ambient temperatures are high and radiation incidence angles are favorable. In contrast, performance significantly decreases during the winter and morning hours due to weak radiation and low temperatures.

These results indicate the importance of integrating the dryer's technical design (number of collectors, tilt angle, thermal insulation) with external environmental factors (climatic conditions, timing of use, season) to achieve the highest thermal efficiency and reduce drying time. Therefore, the adoption of solar dryers in local agricultural systems can contribute to reducing dependence on traditional energy sources, improving the quality of dried products, and enhancing the environmental and economic sustainability of the agricultural sector.

REFERENCE

[1] A. R. Caparanga, R. A. L. Reyes, R. L. Rivas, F. C. De Vera, V. Retnasamy, and H. Aris, "Effects of air temperature and velocity on the drying kinetics and product particle size of starch from arrowroot (Maranta arundinacae)," EPJ Web Conf., vol. 162, pp. 4–8, 2017, doi: 10.1051/epjconf/201716201084.

[2] C. Romaissa, "Réalisation Et Expérimentation D'un Système De Séchage Solaire Pour Le Produit Agro-alimentaire," UNIVERSITE SAAD DAHLEB BLIDA, 2023.

[3] B. Yahia and G. M. Abdelghani, "Développement d'un système de séchage Intelligent Présenté," U N I V E R S I T E Y A H I A F A R E S D E M E D E A, 2021.

[4] K. G. Harding, "Heat Transfer Introduction," Res. Gate, no. September, p. 65, 2021, doi: publication/323144799.

[5] S. Bachir, "Modélisation mathématique de séchage solaire indirect des dattes Deglet-Nour réhumidifiées," UNIVERSITE KASDI MERBAH OUARGLA, 2015.

[6] T. B. Abdelouahed, MESAI AHMED, "Etude expérimentale du séchage solaire des produits agro- alimentaires de la région d'el-oued, mémoire master," Université Echahid Hamma Lakhdar d'El-Oued, 2013.

[7] Slimane BOUGHALI, "ETUDE ET OPTIMISATION DU SECHAGE SOLAIRE DES PRODUITS AGRO-ALIMENTAIRES DANS LES ZONES ARIDES ET DESERTIQUES," UNIVERSITE HADJ LAKHDAR BATNA, 2010.

[8] R. Fortunatus, R. Marealle, N. Nenguwo, and T. Stoilova, "Solar Dryers PRINCIPLES AND BASICS," world vegetqble Cent., p. 27, 2017.

[9] F. Chichango, L. Cristóvão, P. Muguirima, and S. Grande, "Solar dryer technologies for agricultural products in Mozambique: An overview," Res. Soc. Dev., vol. 12, no. 4, p. 9, 2023, doi: 10.33448/rsd-v12i4.39850.

[10] A. B. Lingayat, V. P. Chandramohan, V. R. K. Raju, and V. Meda, "A review on indirect type solar dryers for agricultural crops – Dryer setup, its performance, energy storage and important highlights," Appl. Energy, vol. 258, p. 114005, 2020, doi: https://doi.org/10.1016/j.apenergy.2019.114005.

[11] M. Z. Rahman and M. Hasanuzzaman, "Chapter 8 - Solar drying system," M. B. T.-T. for S. T. E. Hasanuzzaman, Ed., Academic Press, 2022, pp. 237–266. doi: https://doi.org/10.1016/B978-0-12-823959-9.00010-6.

[12] A. Sharma, C. Chen, and N. Lan, "Solar-energy drying systems: A review," Renew. Sustain. Energy Rev., vol. 13, pp. 1185–1210, Aug. 2009, doi: 10.1016/j.rser.2008.08.015.

[13] T. S. S. Bhaskara Rao and S. Murugan, "Solar drying of medicinal herbs: A review," Sol.

Energy, vol. 223, pp. 415–436, 2021, doi: https://doi.org/10.1016/j.solener.2021.05.065.
[14] L. Fernandes and P. B. Tavares, “A Review on Solar Drying Devices: Heat Transfer, Air Movement and Type of Chambers,” Solar, vol. 4, no. 1, pp. 15–42, 2024, doi: 10.3390/solar4010002.
[15] A. A. El-Sebaii and s Shalaby, “Solar drying of agricultural products: A review,” Renew. Sustain. Energy Rev. - RENEW Sustain ENERGY REV, vol. 16, Jan. 2012, doi: 10.1016/j.rser.2011.07.134.
[16] H. Karami et al., “Thermodynamic evaluation of the forced convective hybrid-solar dryer during drying process of rosemary (Rosmarinus officinalis l.) leaves,” Energies, vol. 14, no. 18, p. 16, 2021, doi: 10.3390/en14185835.
[17] Centurion University, “Drying Theory and Principles,” Courseware, 2020.
[18] A. E. E, M. H, and W. Qu, “Influence of Air Temperature on the Drying Kinetics and Quality of Tomato Slices,” J. Food Process. Technol., vol. 02, no. 05, 2011, doi: 10.4172/2157-7110.1000123.
[19] M. Leon, S. Kumar, and S. Bhattacharya, “A comprehensive procedure for performance evaluation of solar food dryers,” Renew. Sustain. Energy Rev., vol. 6, pp. 367–393, Aug. 2002, doi: 10.1016/S1364-0321(02)00005-9.
[20] M. D. Kahina, “Dimensionnement et Réalisation d’une Serre Solaire Destinée pour le Séchage des Déchets Alimentaires,” UNIVERSITE SAAD DAHLEB DE BLIDA FACULTE, 2013.
[21] T. T. Boroze, “OUTIL D’AIDE A LA CONCEPTION DE SECHOIRS POUR LES PRODUITS AGRICOLES TROPICAUX,” PRESENTÉE POUR OBTENIR LE GRADE DE DOCTEUR DE L’UNIVERSITE de LOME, 2011.
[22] S. Nabnean and P. Nimnuan, “Experimental performance of direct forced convection household solar dryer for drying banana,” Case Stud. Therm. Eng., vol. 22, p. 100787, 2020, doi: https://doi.org/10.1016/j.csite.2020.100787.
[23] A. Tefera, W. Endalew, and B. Fikiru, “Evaluation and demonstration of direct solar potato dryer,” Livest. Res. Rural Dev., vol. 25, pp. 1–15, 2013.
[24] J. Ennissioui, E. M. Benghoulam, and T. El Rhafiki, “Experimental study of a natural convection indirect solar dryer,” Heliyon, vol. 9, no. 11, p. e21299, 2023, doi: https://doi.org/10.1016/j.heliyon.2023.e21299.
[25] R. Ben Slama and M. Combarnous, “Study of orange peels dryings kinetics and development of a solar dryer by forced convection,” Sol. Energy, vol. 85, no. 3, pp. 570–578, 2011, doi: https://doi.org/10.1016/j.solener.2011.01.001.
[26] S. Shamekhi-Amiri, T. B. Gorji, M. Gorji-Bandpy, and M. Jahanshahi, “Drying

behaviour of lemon balm leaves in an indirect double-pass packed bed forced convection solar dryer system," Case Stud. Therm. Eng., vol. 12, pp. 677–686, 2018, doi: https://doi.org/10.1016/j.csite.2018.08.007.
[27] N. Khan, K. Sudhakar, and R. Mamat, "Seaweed processing: efficiency, kinetics, and quality attributes under solar drying," Food Chem. Adv., vol. 6, p. 10, Mar. 2025, doi: 10.1016/j.focha.2024.100859.
[28] A. Jain, M. Sharma, A. Kumar, A. Sharma, and A. Palamanit, "Computational fluid dynamics simulation and energy analysis of domestic direct-type multi-shelf solar dryer," J. Therm. Anal. Calorim., vol. 136, pp. 173–184, 2018, doi: 10.1007/s10973-018-7973-5.
[29] O. I. Alonge and S. O. Obayopo, "Computational fluid dynamics and experimental analysis of direct solar dryer for fish," Agric. Eng. Int. CIGR J., vol. 21, no. 2, pp. 108–117, 2019.
[30] F. Afshari, A. D. Tuncer, A. Sözen, E. Çiftçi, and A. Khanlari, "Experimental and numerical analysis of a compact indirect solar dehumidification system," Sol. Energy, vol. 226, pp. 72–84, 2021, doi: https://doi.org/10.1016/j.solener.2021.08.025.
[31] A. Ricaud, "Gisement solaire," Cythelia Sarl, Sept., 2009.
[32] D. Patel and B. Patel, "Low Cost and Robust Solar Tracking System Based On Data of Daily and Seasonal Variation in Sun Position Regard to Specific Location on Earth," Int. J. Innov. Res. Sci. Eng. Technol., vol. 3, pp. 15888 – 15893, 2014, doi: 10.15680/IJIRSET.2014.0309014.
[33] "SOLIDWORKS 3D CAD." [Online]. Available: https://www.solidworks.com/product/solidworks-3d-cad
[34] P. J. Schilling and R. H. Shih, Parametric Modeling with SOLIDWORKS 2025. SDC Publications, 2025.
[35] C. D. C. P. Marie P. Planchard, "Engineering Design with SolidWorks 2012," 2012.
[36] J. Chahed, "Chapitre 7 : Equations de Navier Stokes et écoulements de référence," 2022. doi: 10.13140/RG.2.2.10320.38405.
[37] "URAER - CDER Unié de Recherche Appliquée en Energies Renouvelables." [Online]. Available: http://uraer.cder.dz/

الجمهورية الجزائرية الديمقراطية الشعبية
وزارة التعليم العالي والبحث العلمي

Université de Ghardaia
Faculté des Sciences et de la Technologie

جامعة غرداية
كلية العلوم والتكنولوجيا

غرداية في : 1...../1...../2025

شهادة ترخيص بالتصحيح والايداع:

انا الاستاذ(ة) .....

بصفتي المشرف المسؤول عن تصحيح مذكرة تخرج (ليسانس/ماستر/دكتورا) المعنونة بـ

.....

من انجاز الطالب (الطلبة):

.....

.....

الذي نوقشت/قيمت بتاريخ : .....

اشهد ان الطالب/الطلبة قد قام /قاموا بالتعديلات والتصحيحات المطلوبة من طرف لجنة المناقشة وقد تم التحقق من ذلك من طرفنا

وقد استوفت جميع الشروط المطلوبة .

مصادقة رئيس القسم

امضاء المسؤول عن التصحيح